

5 Visibility Modeling Using Continuous Aerosol Size Distribution Monitors

5.1 Introduction

The fact that severe visibility reduction occurs in the Los Angeles area atmosphere is one of the most widely recognized effects of air pollution. On about 25 percent of the days of the summer months, visual range is reduced to less than 9 km at midday in Southern California communities such as San Bernardino and Upland, and to less than 11 km in Pasadena (Larson and Cass, 1989). A number of special studies have been conducted in the past to demonstrate that visibility phenomena in the Los Angeles area can be connected to air pollutant properties, including aerosol chemical composition, relative humidity, and aerosol size distributions. Empirical models that use aerosol chemical composition and relative humidity data as surrogates for aerosol size and solubility have been formulated and tested (White and Roberts, 1977; Cass, 1979; Trijonis, 1980). Such models have shown that sulfate and nitrate aerosols are important determinants of local visibility reduction. Empirical models of this sort can be supported by aerosol composition data collected by routine air monitoring networks.

More recent studies by Larson *et al.* (1988) have shown that visibility models based directly on Mie theory calculations can be used to describe local visibility reduction phenomena. These models show that aerosol carbon species in addition to sulfates and nitrates play an important role in governing light scattering and absorption in the Southern California atmosphere. Such models based on Mie theory require both a complete chemical analysis of the aerosol samples taken over short periods of time (eg. 4-hr averages or shorter) accompanied by detailed aerosol size distribution measurements. Such data are not at present available on a routine basis from governmental air monitoring networks. The question is then posed, "Is it feasible to operate a routine air monitoring network that supplies data sufficient to support the characterization of regional visibility problems via visibility models based on Mie theory calculations?"

During the summer and fall of 1987, an air monitoring network designed in part to answer that question was deployed in the Los Angeles area as part of the Southern California Air Quality Study (SCAQS). Filter-based sampling to determine aerosol mass concentration and chemical properties in two particle size ranges ($d_p < 2.5 \mu\text{m}$; $d_p < 10 \mu\text{m}$) was conducted over consecutive 4-hour time periods during 8 air pollution episodes covering 17 different days (see Table 1). Aerosol size distributions were measured continuously using electrical aerosol analyzers (EAA) and optical particle counters (OPC) at the Claremont, Long Beach, Rubidoux, and Central Los Angeles sites shown in Figure 1 on the dates shown in Table 1. Integrating nephelometers were used to measure the aerosol scattering coefficient at each site. This combination of aerosol size distribution data derived from automated operation of EAA's and OPC's plus filter based aerosol chemical data from which particle solubility and refractive index values can be estimated probably constitutes the least expensive combination of routine measurements that could be employed to meet the input data requirements of visibility models based on Mie theory calculations. In the present report, we explore the accuracy with which the time series of SCAQS air monitoring network data can be used to account for the time series of atmospheric light scattering coefficient values from Mie theory calculations via the methods proposed by Larson and Cass (1989).

5.2 Experimental Program

The overall design of the Southern California Air Quality Study experiments is described by Blumenthal *et al.* (1986) and Hering *et al.* (1989). Only those aerosol characterization experiments important to the present work will be recounted here.

5.2.1 SCAQS Sampling

The SCAQS field program ran for nine weeks in the summer and four weeks in the fall of 1987. During these periods, several one to three day episodes were selected for intensive sampling. The field study included a network of 36 existing governmental routine air quality monitoring stations (C sites), six to nine monitoring stations located along typical air

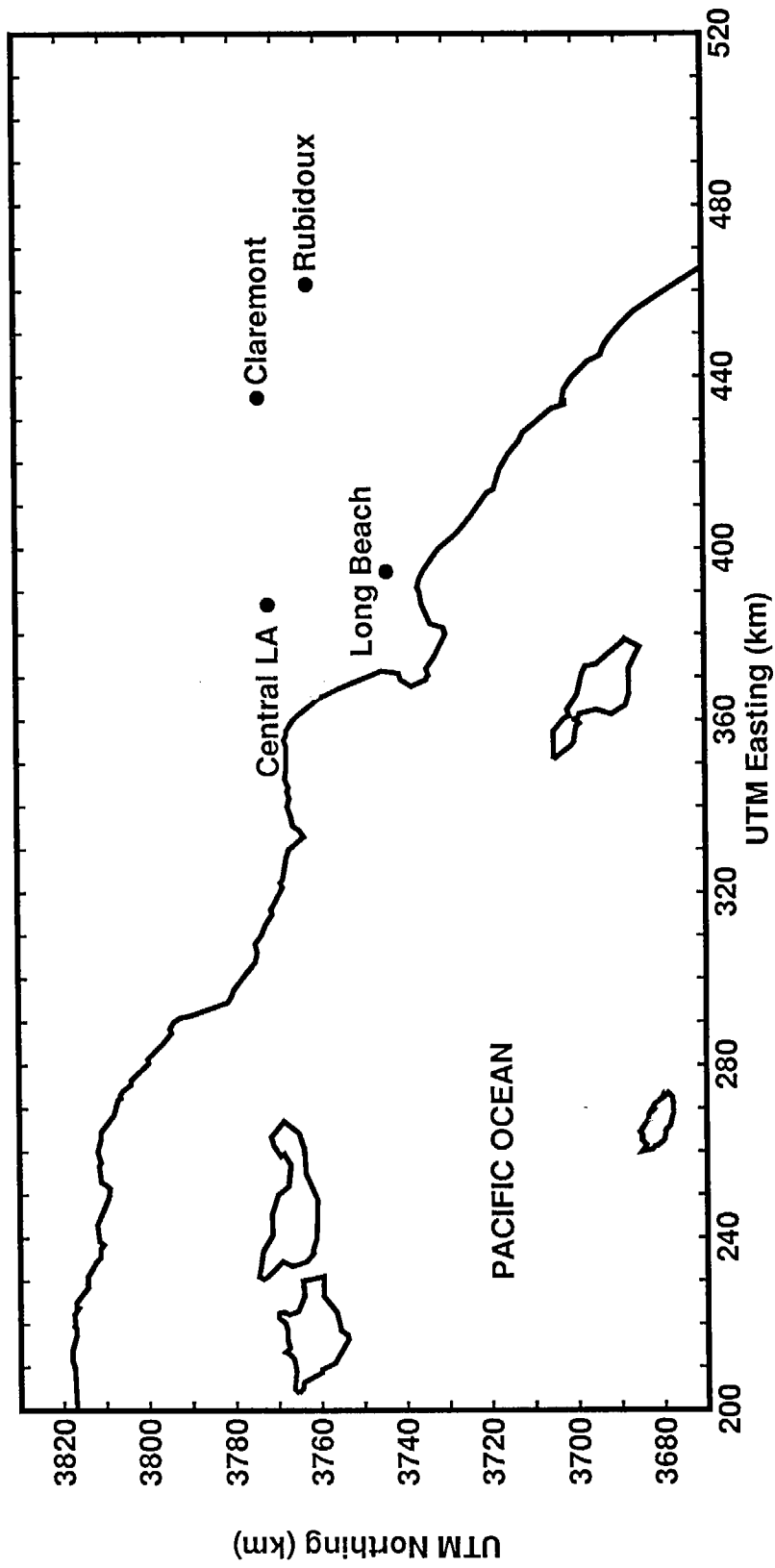


Figure 1: Southern California showing the locations of the aerosol size distribution monitoring network operated during SCAQS.

Table 1: Sites and Dates of SCAQS Intensive Field Experiments

<i>Sites</i>	<i>Location</i>	<i>station type</i>					
		summer			fall		
		B	B ⁺	A	B	B ⁺	A
Claremont	Claremont McKenna College	✓	✓	✓			
Long Beach	Long Beach City College	✓	✓	✓	✓	✓	✓
Rubidoux	SCAQMD Monitoring Station	✓	✓		✓		
Central LA	SCAQMD Monitoring Station	✓			✓	✓	
1987 summer dates:		June 19, June 24-25, July 13-15 August 27-29, September 02-03					
1987 fall dates:		November 11-13, December 03, December 10-11					

trajectories where routine monitoring for aerosols and gases was enhanced by special instrumentation on intensive study days (B sites), and one or two stations in source and receptor regions where research scientists employed highly specialized equipment that was not available as part of monitoring network operations (A sites) (Chan and Durkee, 1989). At four of the air monitoring network B sites aerosol size distribution measurements were made (B⁺ sites). During the SCAQS summer and fall 1987 intensive periods, AeroVironment, Inc. was responsible for operating the SCAQS network (SC) aerosol instruments on the SCAQS intensive dates shown in Table 1. Aerosol size distribution measurements were made at the Claremont, Rubidoux, and Long Beach sites during the summer, and at the Long Beach and Central Los Angeles sites during the fall experiments.

The majority of the SCAQS data required for the present visibility modeling study are in good order. The following sections will describe the data being used and any notable limitations of the data base. A number of documents are available with additional experimental details (Hering *et al.* 1989; Hering, 1990; Matsumura *et al.*, 1991).

5.2.2 Aerosol Size Distributions

Aerosol size distributions were measured using an electrical aerosol analyzer (EAA, TSI Model 3030) for particles from 0.007 μm to 0.32 μm in diameter, a Particle Measuring Systems LAS-X active scattering laser optical counter (PMS OPC) for particles 0.095 to 2.83 μm in diameter, and a Climet 208 white light optical particle counter (Climet OPC) for particles in the diameter range from 0.72 to 9 μm . Data were acquired over consecutive four minute averaging times, and then averaged to one hour periods. Table 2 documents how specific instruments were moved from site to site between the summer and fall experiments.

5.2.3 Aerosol Chemical Composition Measurements

Aerosol mass concentrations and chemical composition were measured using the SCAQS sampler developed for this study by Fitz *et al.* (1989) (see Figure 2). Aerosol samples were taken in two particle size fractions, corresponding to aerodynamic particle diameters of less

Table 2: Identification Numbers of Instruments used in the SCAQS Study Showing the Location of Particular Instruments during Different Seasons of the Year

<i>Site</i>	<i>EAA</i>	<i>PMS OPC</i>	<i>Climet OPC</i>	<i>SC nephelometer</i>
Claremont summer	58	9835-0387-86	76-148	1561/121
Long Beach summer	80	9835-0387-85	76-060	1561/118
Rubidoux summer	97	1118-0679-18	76-065	1561/185
Central LA fall (Nov.)	58	9835-0387-85	76-148	1562/149
Central LA fall (Dec.)	58	9835-0387-86	76-060	1562/149
Long Beach fall	97	1118-0679-18	76-065	1560/128

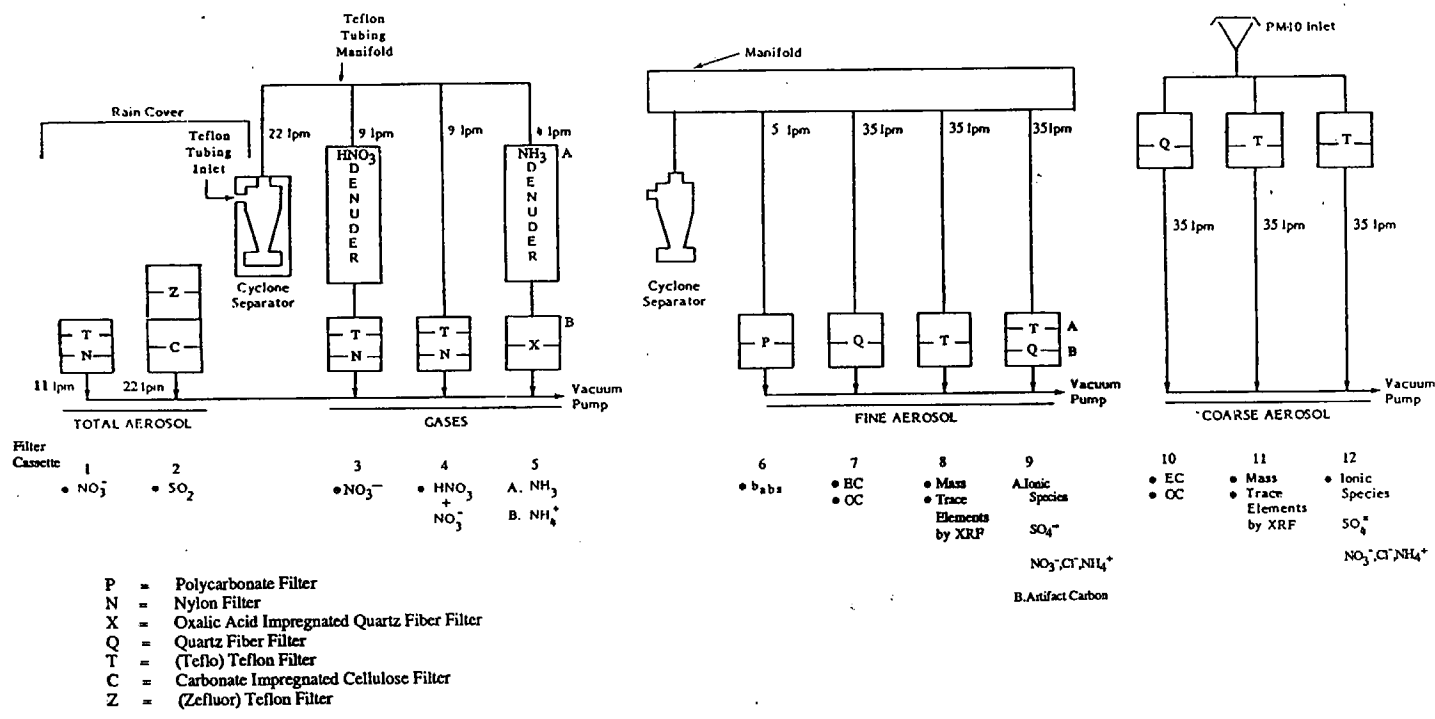


Figure 2: SCAQS sampler used for filter-based measurements of PM2.5 and PM10 aerosol mass concentrations and chemical composition.

than 2.5 μm (PM_{2.5}) and less than 10 μm (PM₁₀). Fine particle (PM_{2.5}) and PM₁₀ samples were collected on 47mm diameter Teflon filters that were then analyzed to determine aerosol mass, trace element, and ionic species concentrations. Samples collected on 47mm pre-fired quartz fiber filters were analyzed for organic and elemental carbon concentrations. A 47mm Nuclepore filter was used for particle light absorption determinations by the integrating plate method. Gravimetric techniques were used to determine the aerosol mass concentrations. Ion chromatography was used to analyze for NO_3^- , SO_4^{2-} , and Cl^- . Ammonium ion concentrations were determined by colorimetry. Atomic absorption spectrophotometry was used to measure PM₁₀ sodium concentrations. Organic and elemental carbon were measured by the dual temperature zone furnace oxidation method by ENSR Corp. (Chan and Durkee, 1989). Trace element concentrations were measured by X-ray fluorescence (XRF), and were corrected for deposit non-uniformity on the filters according to the recommendations of Matsumura and Cahill (1991) .

The SCAQS sampler was used to collect five samples per day on intensive study days, with sampling periods of four hours (daytime) and five to seven hours (nighttime) duration. Samples were changed at 0100, 0600, 1000, 1400, and 1800 hours PDT in the summer, and at 2400, 0600, 1000, 1400, and 1800 hours PST in the fall. These sampling durations are the longest of the measurements needed in the present visibility modeling study, and thus other data will be averaged to match these sampling periods.

An effort was made to account for the possible volatilization of aerosol nitrate and ammonium ion collected on Teflon filters (Appel *et al.*, 1980; Solomon *et al.*, 1988). Along with the Teflon filter samples collected and analyzed for inorganic ions, measurements were made of fine particle nitrate and vapor phase HNO_3 by the denuder difference method (Hering *et al.*, 1988). In this method, air is passed through a 2.5 μm size cut cyclone separator in order to remove coarse particle nitrates. This air stream containing nitric acid vapor and fine aerosol nitrates is then split in half. One half of the flow passes through a HNO_3 diffusion denuder that removes HNO_3 , followed by fine particle nitrate collection on a nylon filter. The second half of the flow is passed directly through a nylon filter, thereby collecting both fine

particle nitrate and HNO_3 . The difference between the nitrate concentrations collected on these two filters is a measurement of the nitric acid concentration, and the aerosol collected downstream of the denuder is thought to represent the true fine particle nitrate concentration. The difference between the fine particle nitrate collected following the HNO_3 denuder and that measured on the fine particle Teflon filter (branch 9 of Figure 2) was taken as an indication of the amount of NH_4NO_3 volatilized from the Teflon filter. This amount was added to both the fine particle and PM_{10} nitrate concentrations as measured on the Teflon filters in sample lines 9 and 12 of Figure 2 along with stoichiometrically equivalent amounts of ammonium ion. The total filter masses were adjusted upwards by the sum of the nitrate and equivalent ammonium ion concentration corrections.

5.2.4 Light Scattering Coefficient Data

Measurements of scattering coefficient values were made at all of the sites listed in Table 1. Particle light scattering coefficient values were measured using SCAQS network (SC) nephelometers by Aerovironment, Inc. or by the South Coast Air Quality Management District (SCAQMD). Meteorology Research, Inc. (MRI) 1560's series nephelometers with heated inlets were used by those two organizations at all sites except Rubidoux. These instruments were calibrated to read zero when observing only Rayleigh scattering by air molecules, thereby measuring only the scattering of light due to particles. These instruments are most sensitive at a wavelength of 525 nm (Ruby and Waggoner, 1981). Scientists from the University of Illinois (UI) (Claremont and Rubidoux, summer) and General Motors Research Laboratories (GM) (Claremont in summer and Long Beach in fall) also collected light scattering data using slightly different instrumentation. The instrumentation used by GM was a MRI 1550 nephelometer with heated inlet, which is most sensitive at 475 nm (Ruby and Waggoner, 1981). The UI data were collected from two temperature programmed nephelometers (Rood *et al.*, 1987). These nephelometers were geometrically similar to MRI 1590 nephelometers, which are most sensitive at 525nm.

Duplicate light scattering data sets were available for the summer period at Claremont

(SC, UI, and GM) and the fall period at Long Beach (SC and GM) as shown in Figure 3. The similarities and differences between the measurements are interesting. The SC and UI measurements are made at the same wavelength, but the SC nephelometer had an inlet that was heated continuously, whereas the UI data used here are taken under ambient temperature conditions. A comparison of these data show that the scattering coefficient reported by SC is consistently smaller than that reported by UI. The heated inlet would be expected to be responsible for some of this result, as the objective of a heated nephelometer is to measure the light scattering by dry particles (ie, following removal of aerosol water). The instrument used by SC is most sensitive at 525nm, and the instrument used by GM is most sensitive at 475nm. Light scattering by atmospheric particles is wavelength dependent, with the light scattering greater at 475 nm than at 525 nm (Middleton, 1952). A comparison of the GM and UI data at Claremont shows that this expected ordering of the data is reflected in the data base most of the time. The scattering coefficient values measured by GM are almost always larger than the values reported by SC, frequently by more than the factor of about 1.1 that would be expected with measurements made at 475 and 525 nm. At Long Beach, half of the scattering coefficient data reported by SC are larger than those reported by GM, and vice versa. These differences seen in simultaneous measurements of the scattering coefficient suggest that not all of the nephelometer measurements at Long Beach can be correct, and that no visibility model can be expected to produce exact agreement with all measured light scattering values because the light scattering data are in conflict to some degree.

5.2.5 Data Base Preparation

Data missing from the SCAQS data base were replaced by closely related measurements where possible. Relative humidity data at the Long Beach SCAQS monitoring site were missing from the SCAQS data set for the summer dates. Relative humidity data collected by the Federal Aviation Administration (FAA) at Dougherty Field in Long Beach was substituted. This air field is 1.7 km (southwest) from the Long Beach City College monitoring site. Some Claremont PM₁₀ NH₄⁺ data that were missing were replaced by estimates obtained

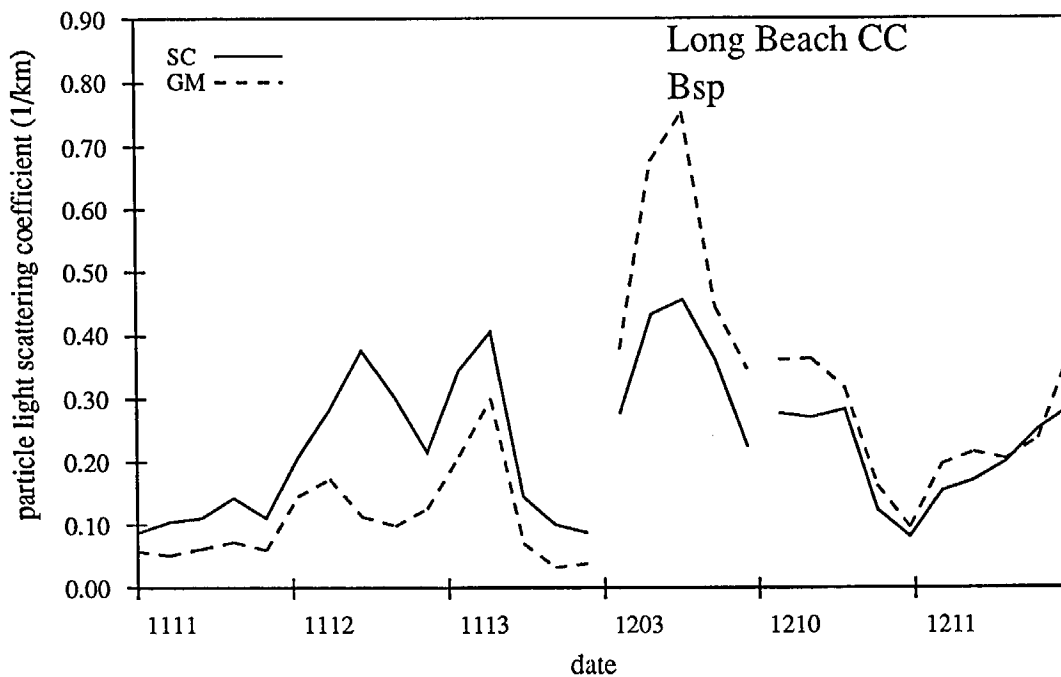
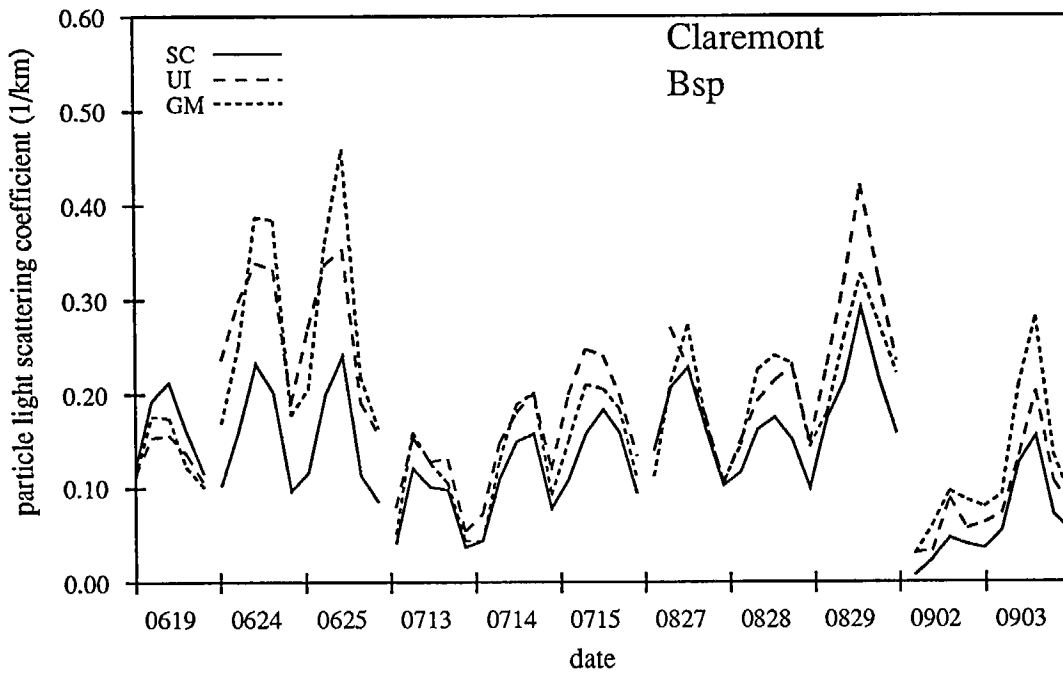


Figure 3: Concurrent measurements of light scattering by particles made by different investigators during SCAQS. Dates are given as month, date (ie., 0619 is June 19, 1987).

from the available fine particle NH_4^+ data via regression of the reported $\text{PM}_{2.5}$ NH_4^+ data on PM_{10} NH_4^+ data at Claremont. This is not expected to lead to significant error since the overwhelming majority of the NH_4^+ was found in fine particles during SCAQS. (The dates and sampling periods where such replacement occurred were August 27, sampling period 5, August 28, all sampling periods, and August 29, sampling periods 1-4.) In four cases, missing data on coarse particle Na^+ concentrations were estimated by completing an ion balance on the PM_{10} samples. This is not expected to lead to appreciable error because, as will be shown later, light scattering by large particles between 2.5 and 10 μm diameter makes only a small contribution to the calculated light scattering coefficient values. In an effort to maximize the days available for modeling, all data that had been marked invalid were examined closely. In some cases chemical data needed solely for the calculation of the refractive index were nearly complete, and the refractive index values were estimated from the available data. At the end of the data base preparation step, all time periods other than those listed in Table 3 contain a set of data on aerosol size distribution, aerosol chemical composition, and temperature sufficient to support light scattering calculations.

5.3 Correction of Aerosol Size Distribution Data Collected by the PMS Optical Particle Counter

Experiments were performed in July of 1987 by Hering and McMurry (1991) to determine the response of a single optical particle counter to monodisperse fractions of Los Angeles area ambient aerosols. Measurements were made at Claremont to calibrate an instrument optically identical to the PMS laser OPC's used in the SCAQS study. The ambient aerosols were found to scatter less light than the polystyrene latex spheres that are used for the factory calibration of these instruments, but about the same amount of light as oleic acid, which has a lower refractive index. Because of this difference in response between atmospheric aerosols and polystyrene latex spheres, these instruments, if used in accordance with the manufacturer's calibration report, will produce an incorrect indication of the atmospheric particle size distribution. Therefore, in the present study, the particle diameters reported

Table 3: Dates and Times with Missing Data

<i>Site</i>	<i>Date</i>	<i>Period</i>	<i>Missing Data</i>
Claremont	0829	1	all size distribution data
Claremont	0829	2	all size distribution data
Rubidoux	0619	2	all aerosol chemistry data
Rubidoux	0625	2	PM2.5 mass missing
Rubidoux	0713	all	PMS OPC data missing
Rubidoux	0714	all	PMS OPC data missing
Long Beach CC	1112	1	all PM2.5 chemistry missing

from the PMS OPC's are corrected according to the results of Hering and McMurry in order to recover the actual size distribution of the atmospheric aerosol. A table showing the conversion factors used to process the PMS OPC data based on Hering and McMurry's (1991) experimental work is included in the appendix to this report.

5.4 Aerosol Volume Distributions

Three aerosol size distribution measurement instruments were deployed at each monitoring site. The size ranges over which each instrument will respond to the ambient aerosol differ, and in some cases measurements made at the tails of the performance range of the instruments may be suspect. In order to examine the degree of agreement between instruments, graphs were drawn comparing the aerosol volume distributions as seen simultaneously by each instrument. Plots were drawn for each hour at each site and for the volume distribution averaged over the sampling periods used for aerosol filter collection. An example is shown in Figure 4. These plots are useful in visualizing similarities and differences between dates and sites. The EAA and PMS laser OPC data are in general agreement over the range of sizes where their response overlaps. The EAA data begin in size ranges well below $0.1 \mu\text{m}$ particle diameter and show that there is little aerosol volume located in particles smaller than $0.1 \mu\text{m}$ diameter. In the particle diameter range from $0.1 \mu\text{m}$ up to about $0.4 \mu\text{m}$ both the EAA and the PMS OPC show that aerosol volume is increasing, reaching a maximum in the value of $dV/d\log d_p$ between about 0.4 to $0.5 \mu\text{m}$ diameter. The PMS OPC with its finer size resolution suggests a distinct mode in the submicron aerosol between 0.1 and $0.3 \mu\text{m}$ followed by a second mode between about 0.3 and $0.6 \mu\text{m}$. Similar bimodal character of the submicron ionic aerosol also has been observed at Claremont by John *et al.* (1990) based on cascade impactor measurements. Above about $0.3 \mu\text{m}$ in diameter, the EAA data cease, while the PMS OPC's generally show a decline in the aerosol volume distribution to low values as the particle diameter examined approaches the upper limit of that instrument at $2.8 \mu\text{m}$. A minimum in the size distribution of Los Angeles area aerosols at about $2 \mu\text{m}$ particle diameter likewise has been observed in many prior studies (Whitby and Sverdrup,

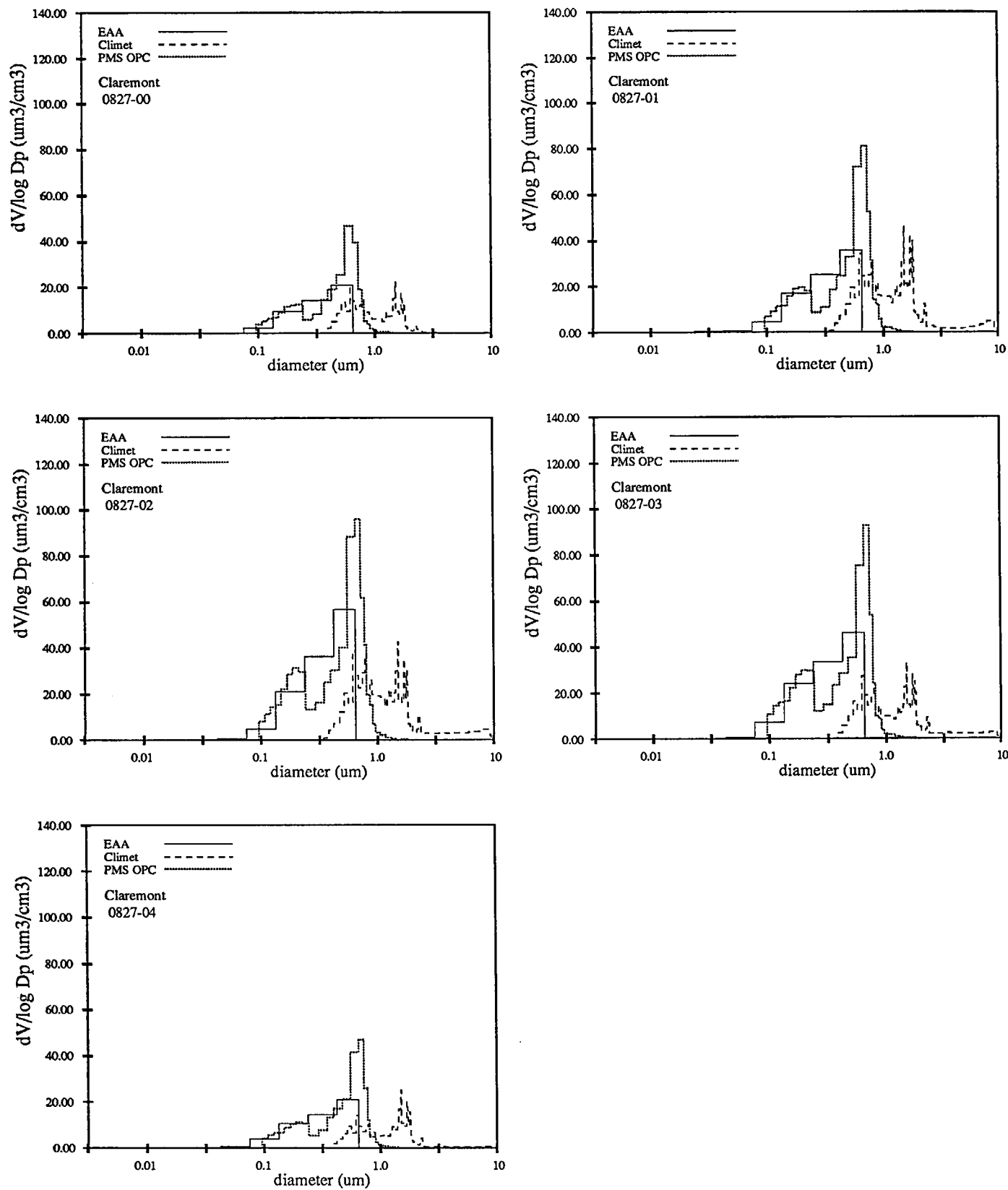


Figure 4: An example of the raw size distribution data from the three size distribution monitors showing the extent of overlap between instruments.

1980; Larson *et al.*, 1988; Wall *et al.*, 1988; John *et al.*, 1990) and forms the basis for the decision to divide fine particles from the rest of the aerosol with a size cut taken at 2.5 μm particle diameter. The Climet white light OPC is not sensitive to the smaller particles counted by the EAA and the PMS OPC, but its range does extend to larger particles (up to 9 μm in diameter). The particle volume distributions drawn from the Climet data typically indicate a greater particle volume than is seen by the PMS OPC in particle sizes larger than about 0.6 μm in diameter. By comparison to prior studies (Larson *et al.*, 1988; Wall *et al.*, 1988; John *et al.*, 1990) and by comparison to the aerosol volume inferred from the difference between PM_{2.5} and PM₁₀ filter samples, the Climet OPC appears to under-report the actual aerosol concentrations present in the range from 2.5 μm to 10 μm particle diameter.

5.5 Creating a Combined Size Distribution for Use in Further Calculations

Aerosol size distributions were created by merging the data from several instruments. The PMS laser OPC nominally reports particle counts over the diameter range from 0.095 μm to 2.83 μm . However, the experiments of Hering and McMurry (1991) provide correction factors for converting the manufacturer's PSL equivalent particle diameters to Los Angeles ambient aerosol equivalent diameters only over the range of sizes larger than 0.2 μm in diameter. Therefore, the smallest particles counted by the PMS OPC's are less well characterized than those at the larger end of that instrument's range of operation. Conversely, the EAA is most reliable at small particle diameters. Consequently, the EAA data were used to describe the aerosol size distribution over the range from 0.007 to 0.23 μm particle diameter while the PMS OPC data were used to describe particles 0.23 μm to 2.83 μm in diameter. While the Climet OPC's nominally measure particles up to 9 μm in diameter, these instruments were frequently found to record very low number counts in the range of 2 to 9 μm particle diameter. Particle mass and volume concentrations in the 2.5 to 10 μm size range obtained from the difference between PM_{2.5} and PM₁₀ filter samples were computed and compared to the Climet data over the same size range. It was found that the Climet instruments significantly underestimated the volume (hence mass) of particles in that size range. As

a result of this finding, the particle size distribution in the diameter range 2.5 to 10 μm was estimated using a constant value of $dV/d\log d_p$ over that diameter range with a total aerosol volume concentration equal to that inferred from the filter data. These relatively large particles are not particularly efficient scatterers of light. It will be shown later that this approximation is suitably accurate for the purposes of the present study. Examples of aerosol size distributions developed in this manner are shown in Figure 5.

5.6 Internal Consistency of the Aerosol Chemistry Data Base

A series of consistency checks were performed on the aerosol chemistry data sets to confirm the quality and usefulness of the data base. Ion balances first were constructed for the water soluble components of each complete aerosol sample. As shown in Figures 6 – 13, the anion versus cation balances on each sample at all sites are in good order, indicating that the data on these important water soluble species are internally consistent.

Next, a material balance was constructed for each aerosol sample in which the sum of the mass concentrations of all chemically identified aerosol species was compared against the gravimetrically measured mass concentration. The procedure used was similar to that of Stelson and Seinfeld (1981), Gray *et al.* (1986), and Larson *et al.* (1988). For each aerosol sampling period at each monitoring site, the measured trace metals were converted to their common oxides according to the schedule shown in Table 4. Organic carbon was multiplied by a factor of 1.4 in order to estimate the mass of organic compounds present. Ionic species concentrations were converted to equivalent ionic compound concentrations by associating anions with cations in the following order: NaCl , $(\text{NH}_4)_2\text{SO}_4$, NH_4NO_3 , NaNO_3 , NH_4HSO_4 , and H_2SO_4 until all ionic species are consumed. Then the estimated trace metals oxides, organic compounds, elemental carbon, and ionic species concentration values are summed. The difference between the gravimetric filter mass and the mass accounted for by specific chemical substances will be referred to as the “residue”.

The total mass of identified chemical species was then compared to the gravimetrically determined filter mass (referred to as measured mass). The average ratio of the sum of the

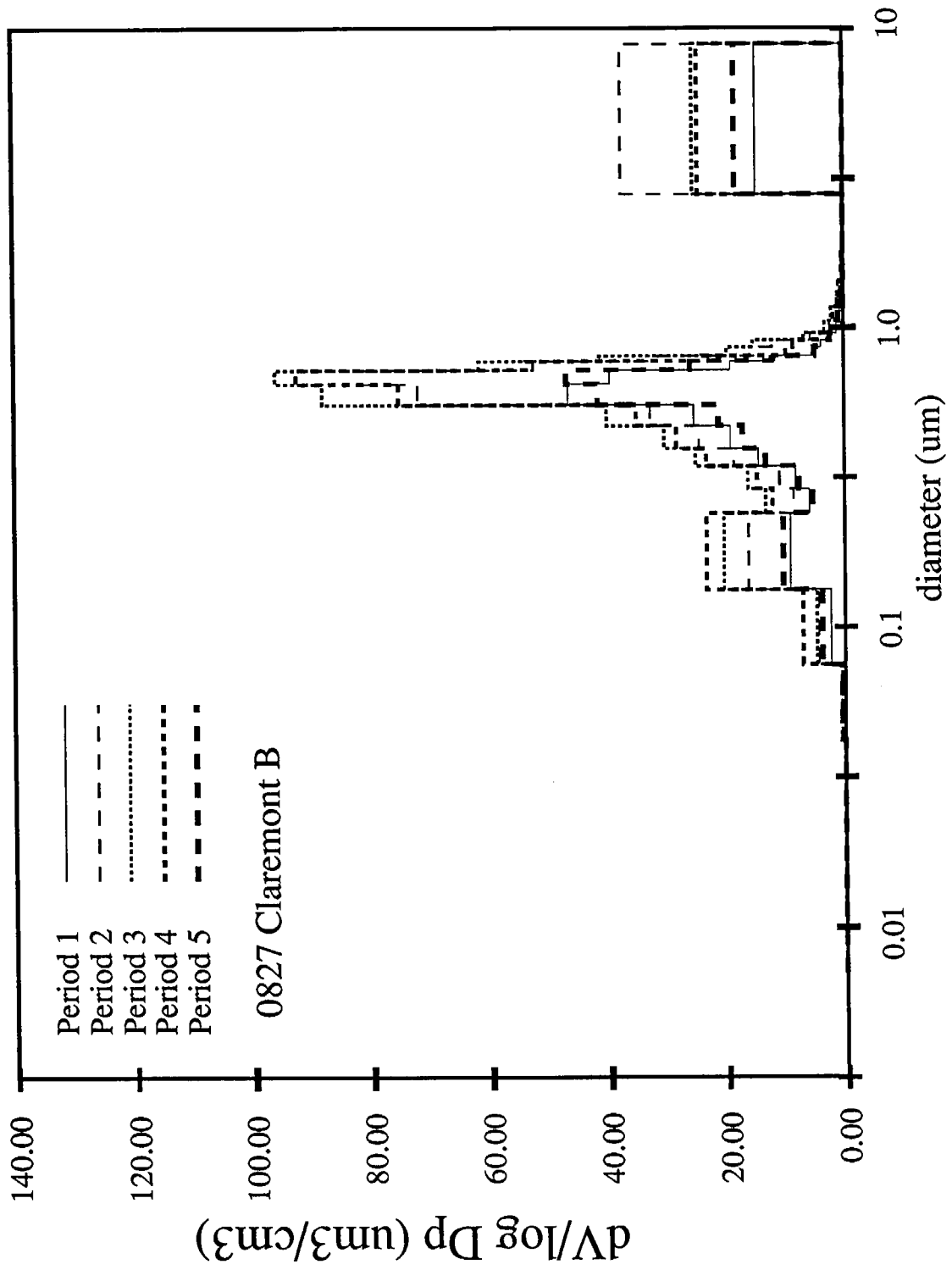


Figure 5: An example of the final aerosol size distribution created for use in visibility modeling.

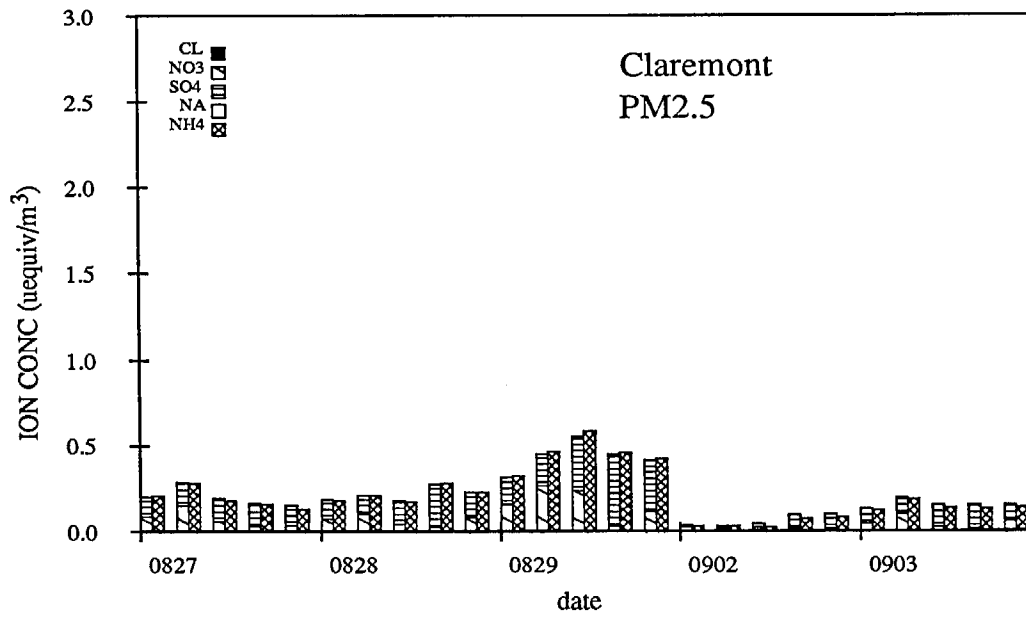
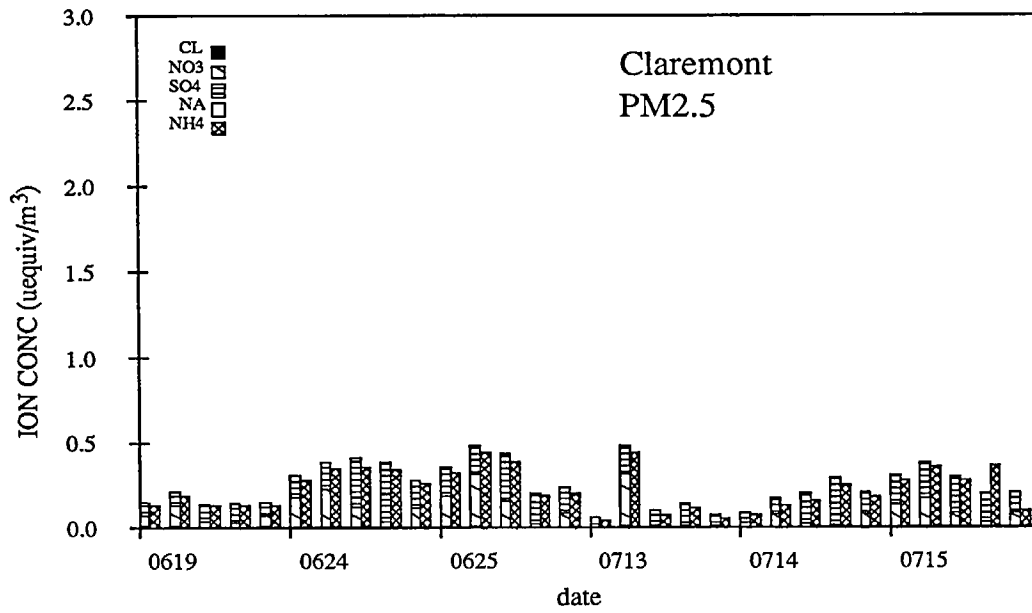


Figure 6: Anion and cation balance for PM_{2.5} at the Claremont site.

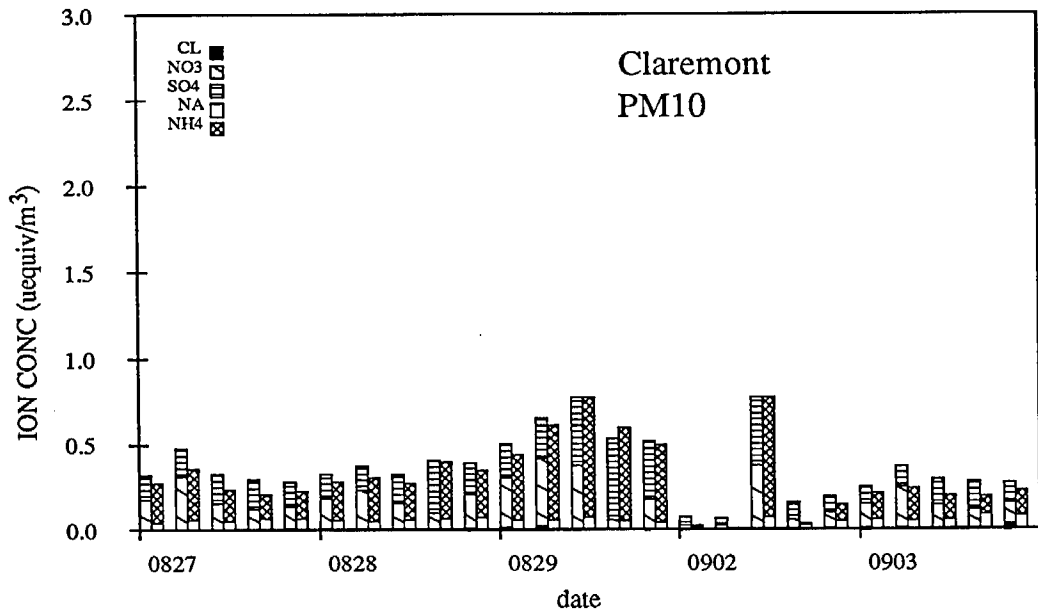
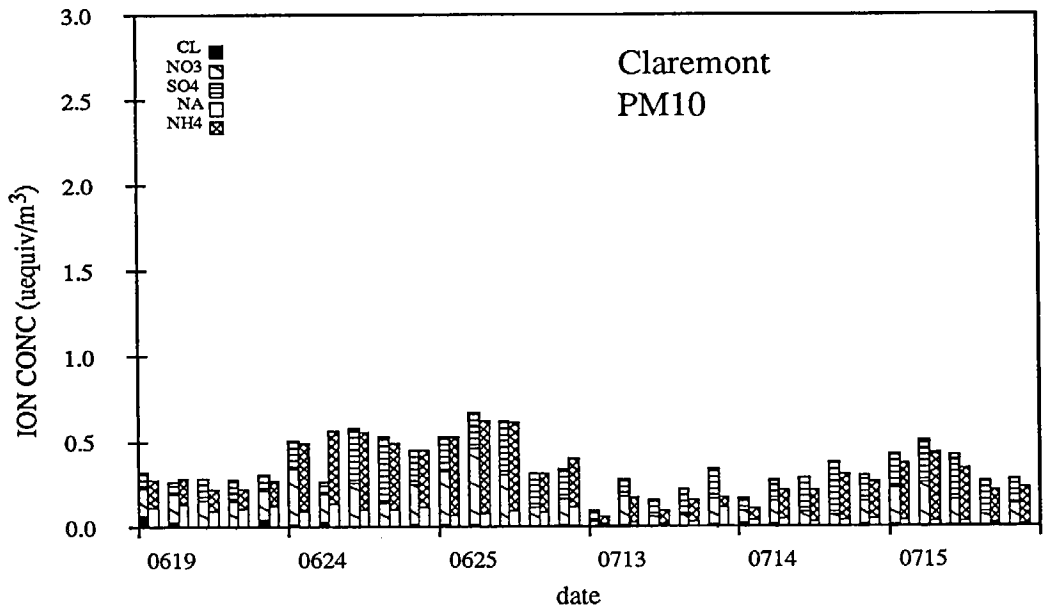


Figure 7: Anion and cation balance for PM10 at the Claremont site.

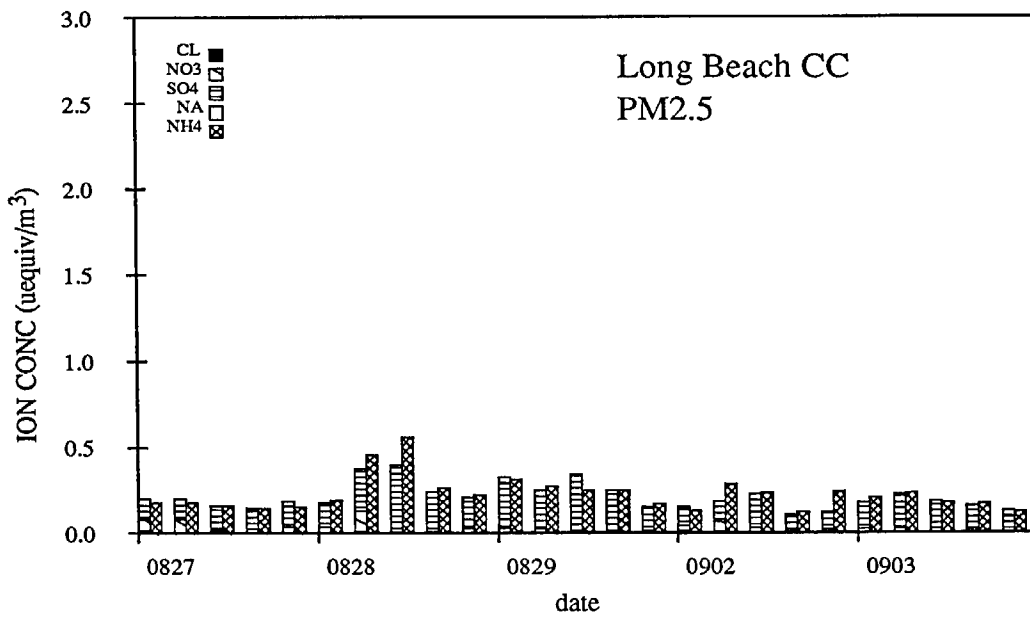
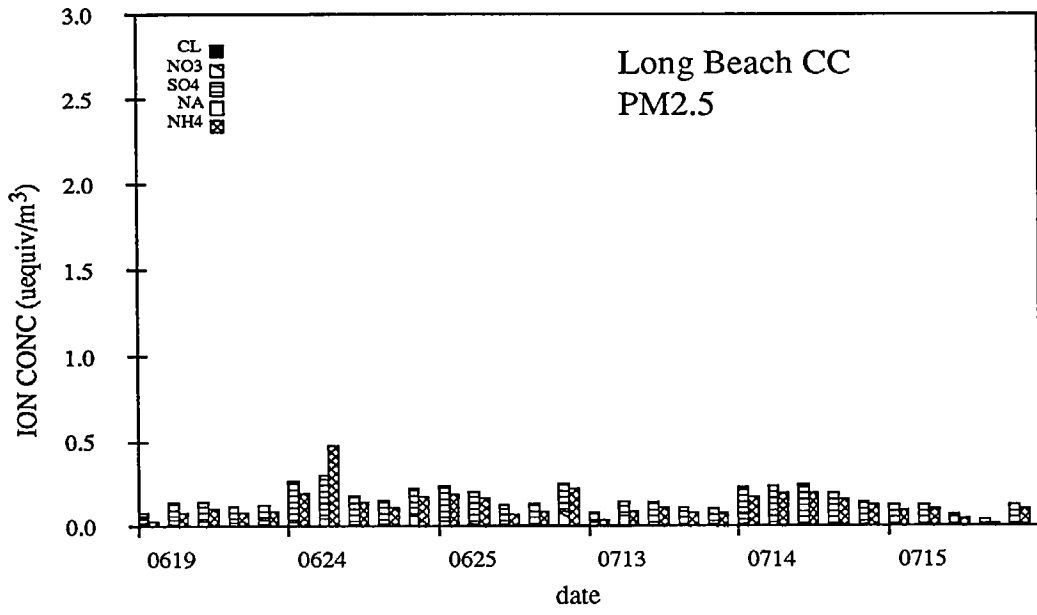


Figure 8: Anion and cation balance for PM2.5 at the Long Beach CC site.

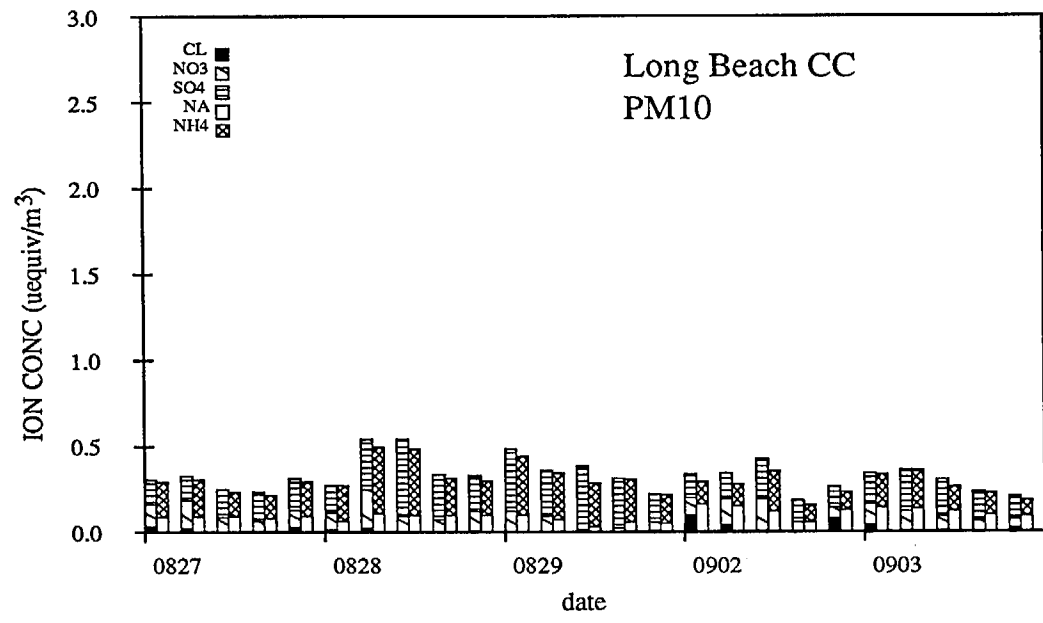
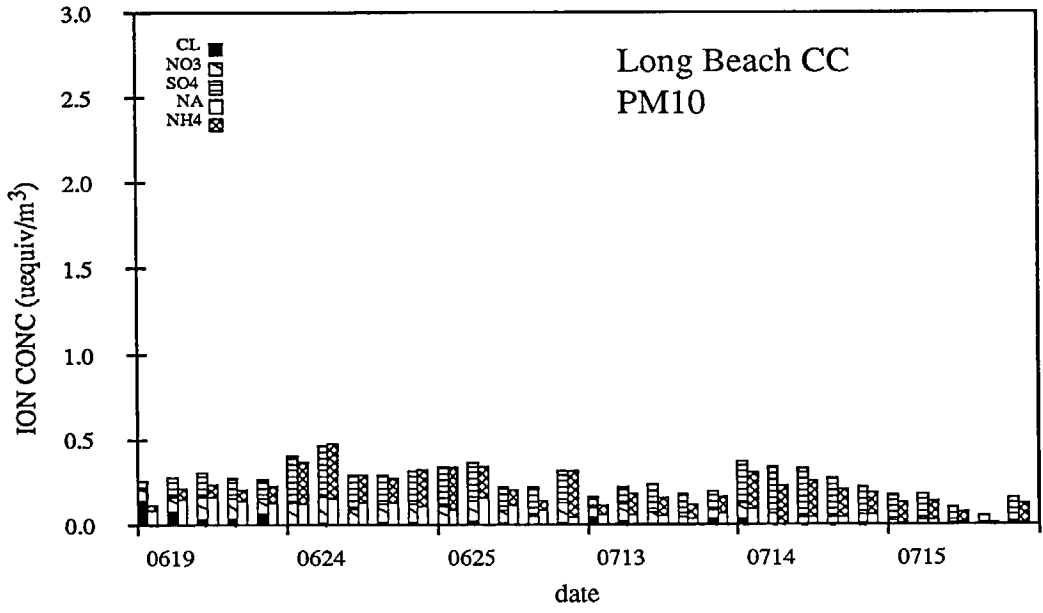


Figure 9: Anion and cation balance for PM10 at the Long Beach CC site.

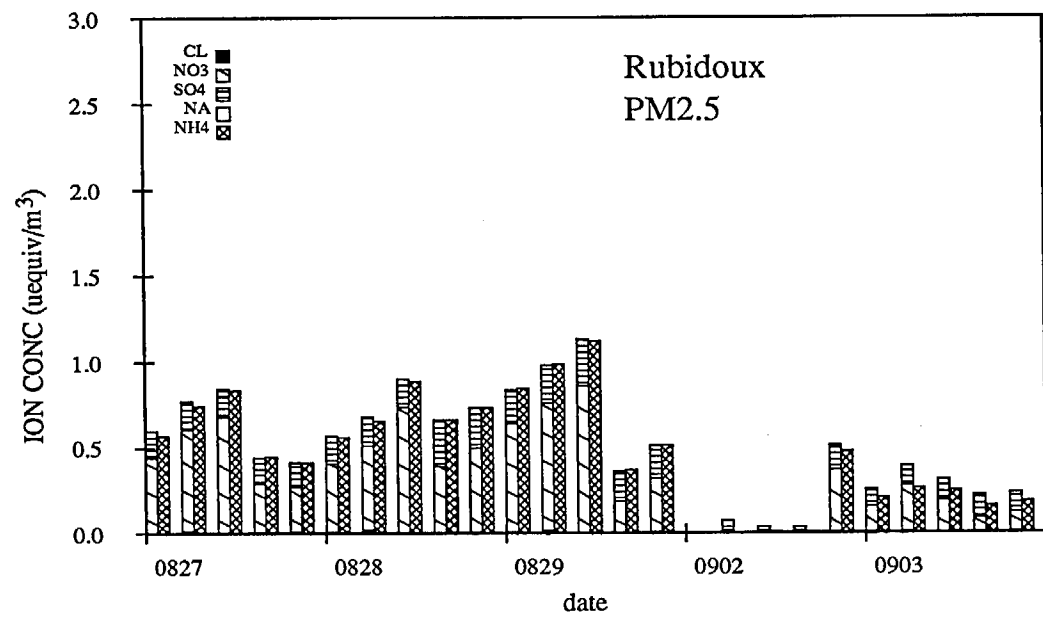
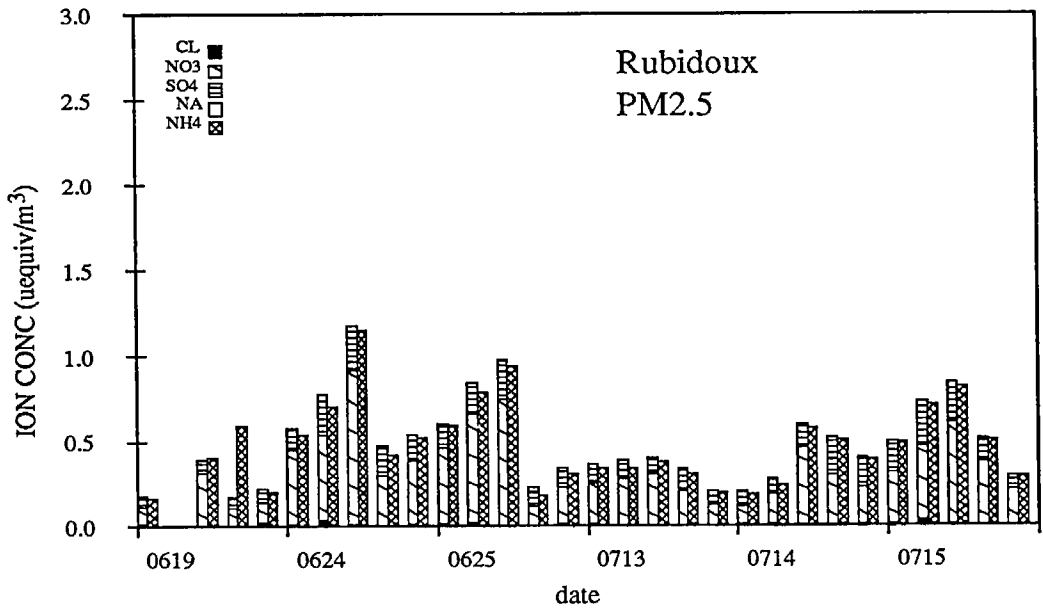


Figure 10: Anion and cation balance for PM2.5 at the Rubidoux site.

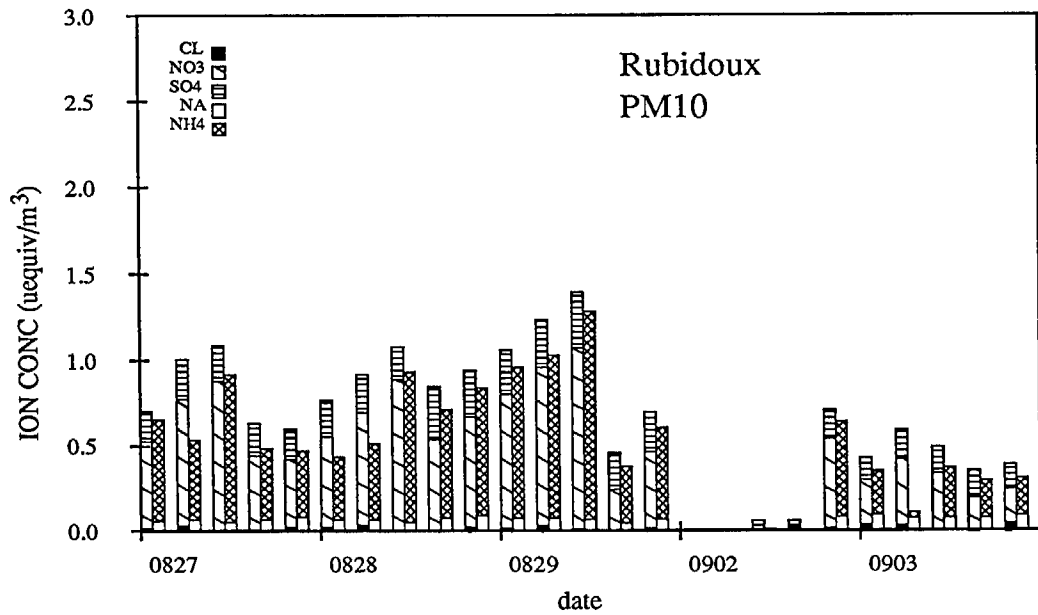
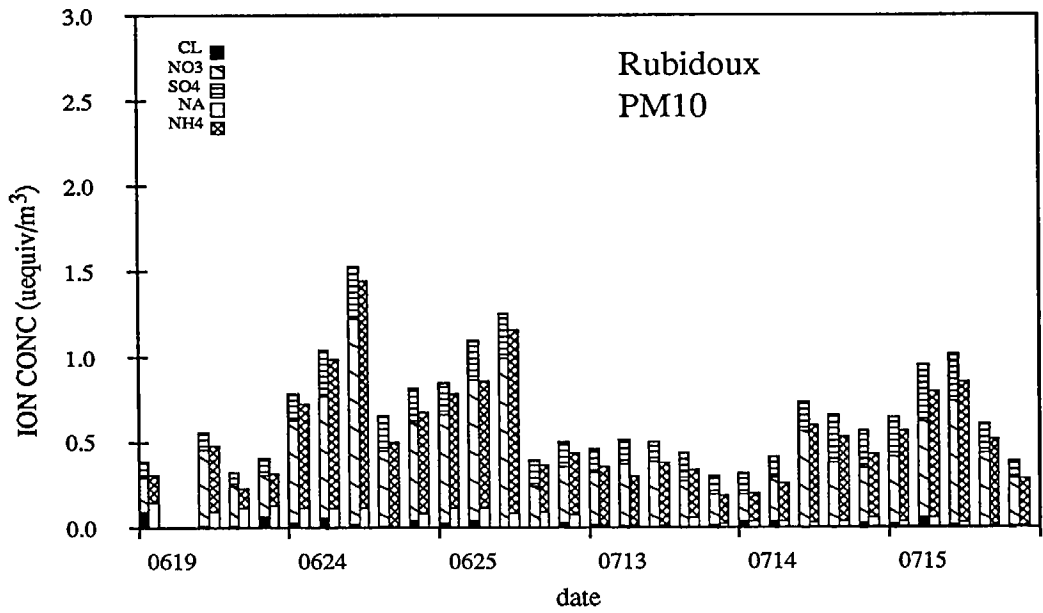


Figure 11: Anion and cation balance for PM10 at the Rubidoux site.

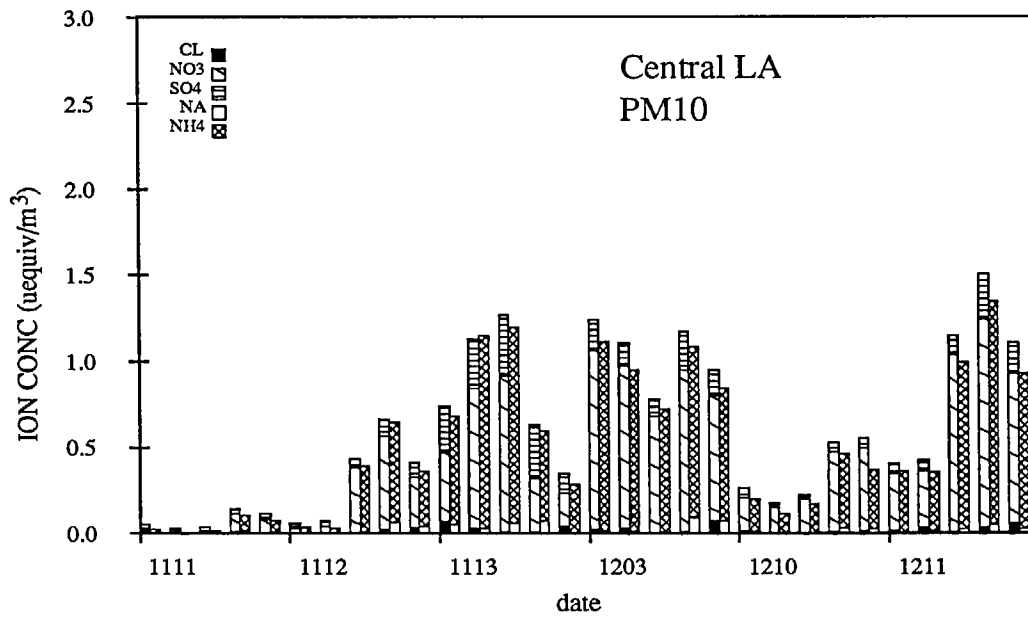
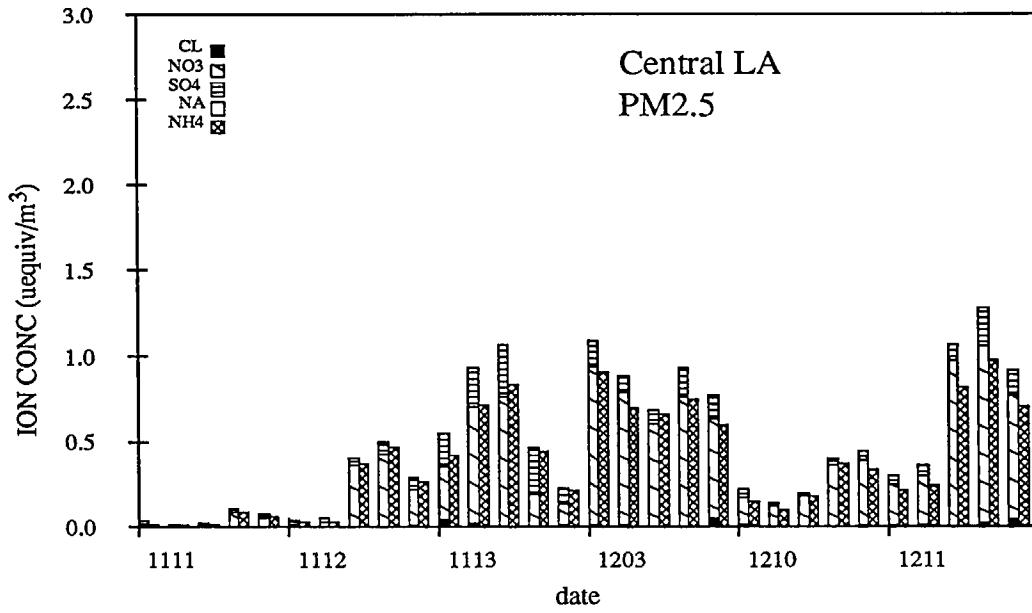


Figure 12: Anion and cation balance for the Central LA site during the fall.

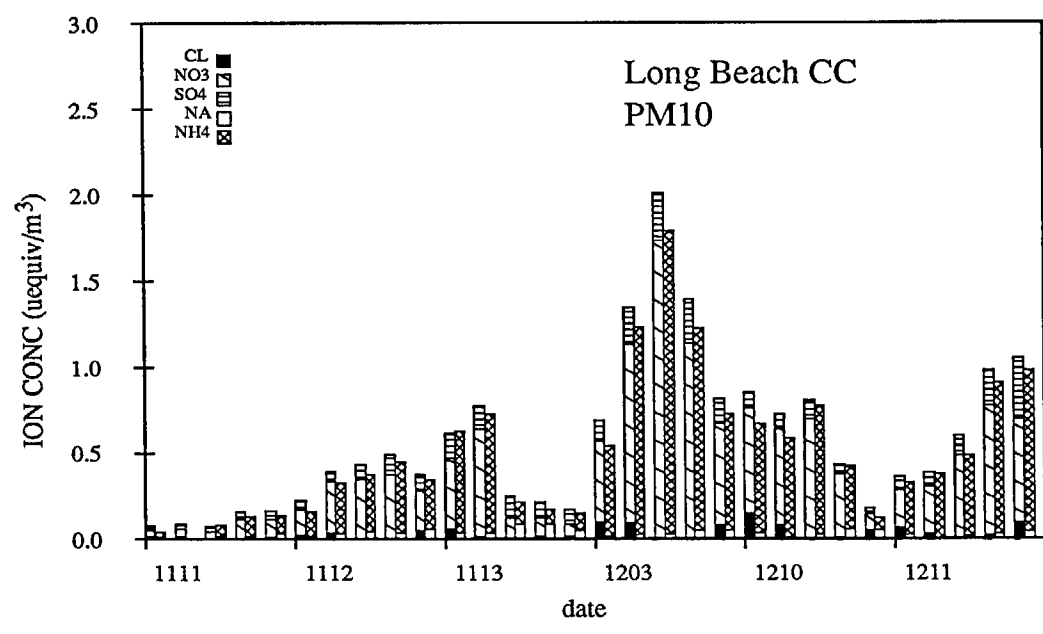
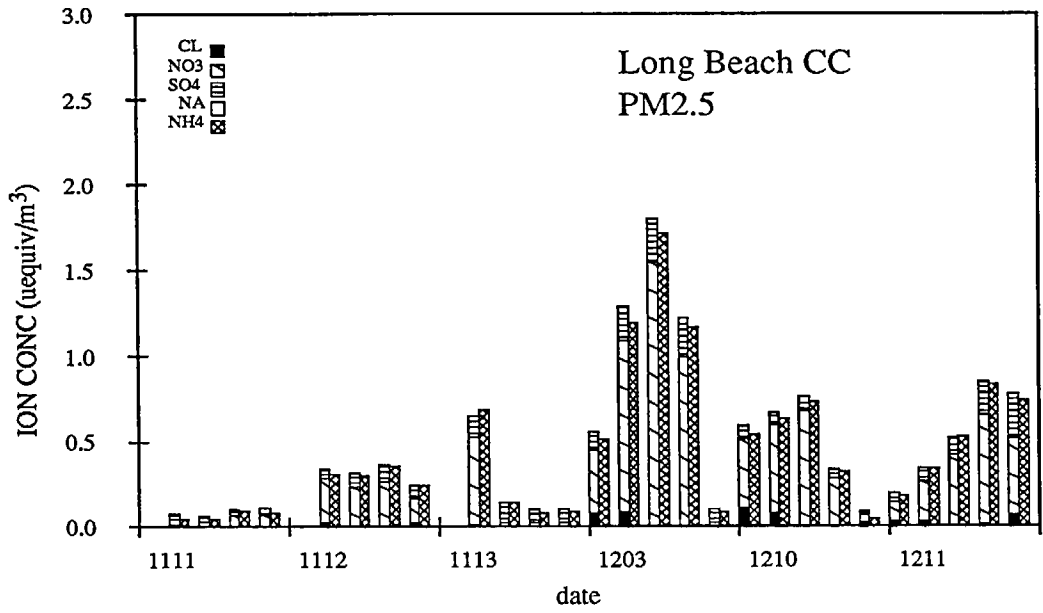


Figure 13: Anion and cation balance for the Long Beach CC site during the fall.

identified individual chemical species to the measured PM_{2.5} filter mass for the summer data at Claremont, Long Beach, and Rubidoux was 0.84, 0.80, and 0.82, respectively, with very few cases of overprediction. For the fall, at Central Los Angeles and Long Beach, the ratio of chemically identified to gravimetrically identified PM_{2.5} filter mass was 0.75 and 0.95 respectively. Material balances on each aerosol sample are shown in Figures 14 and 15.

5.7 Estimation of the Aerosol Liquid Water Content

The gravimetric mass determinations made from filter samples are nominally measured at 45% relative humidity. At such low relative humidity much of the water present in the aerosol under atmospheric conditions has been removed prior to weighing. Prediction of the concentration of aerosol-bound water that is still present at 45% relative humidity is important in order to know the contribution of water to the aerosol mass that is reported after equilibration at low relative humidity.

Comparisons of aerosol volume seen by the size distribution measurement instruments to aerosol volume inferred from the filter data show excellent agreement in most cases. There is no bias that is related to relative humidity, nor any temporal patterns of difference (eg., day/night systematic differences). At all sites, regression of the ratio of aerosol volume measured from the size distribution data to aerosol volume inferred from the filter data on relative humidity yields regression coefficients for the slope that are zero, within the 95% confidence limits. If there was water in the aerosol when the scattering coefficient was measured by the nephelometers, but not when the fine particle mass was measured on the filters, then the ratio of reported fine particle mass concentration to b_{scat} would change as a function of the relative humidity. The relationship between the fine particle mass concentration measured at 45% relative humidity and the measured scattering coefficient was examined graphically and does not show any temporal variations that suggest systematic differences in water content as a function of the time of day. Statistically, Claremont and Rubidoux are the only stations where, with 95% confidence it can be said that regression of the ratio of fine particle mass concentration to b_{scat} on relative humidity produces a

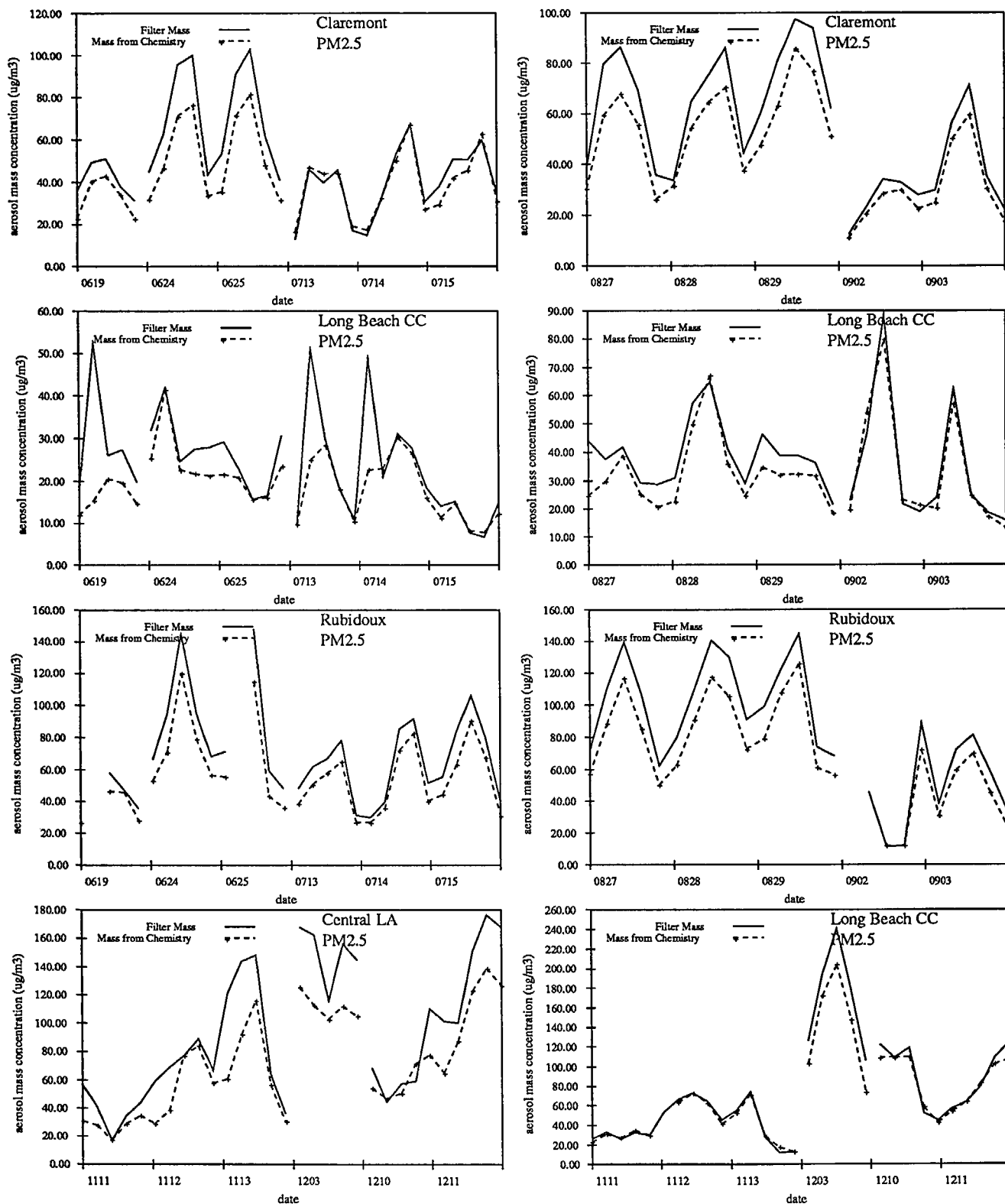


Figure 14: Comparison of gravimetrically determined PM2.5 mass to the sum of the mass concentrations of identified chemical species.

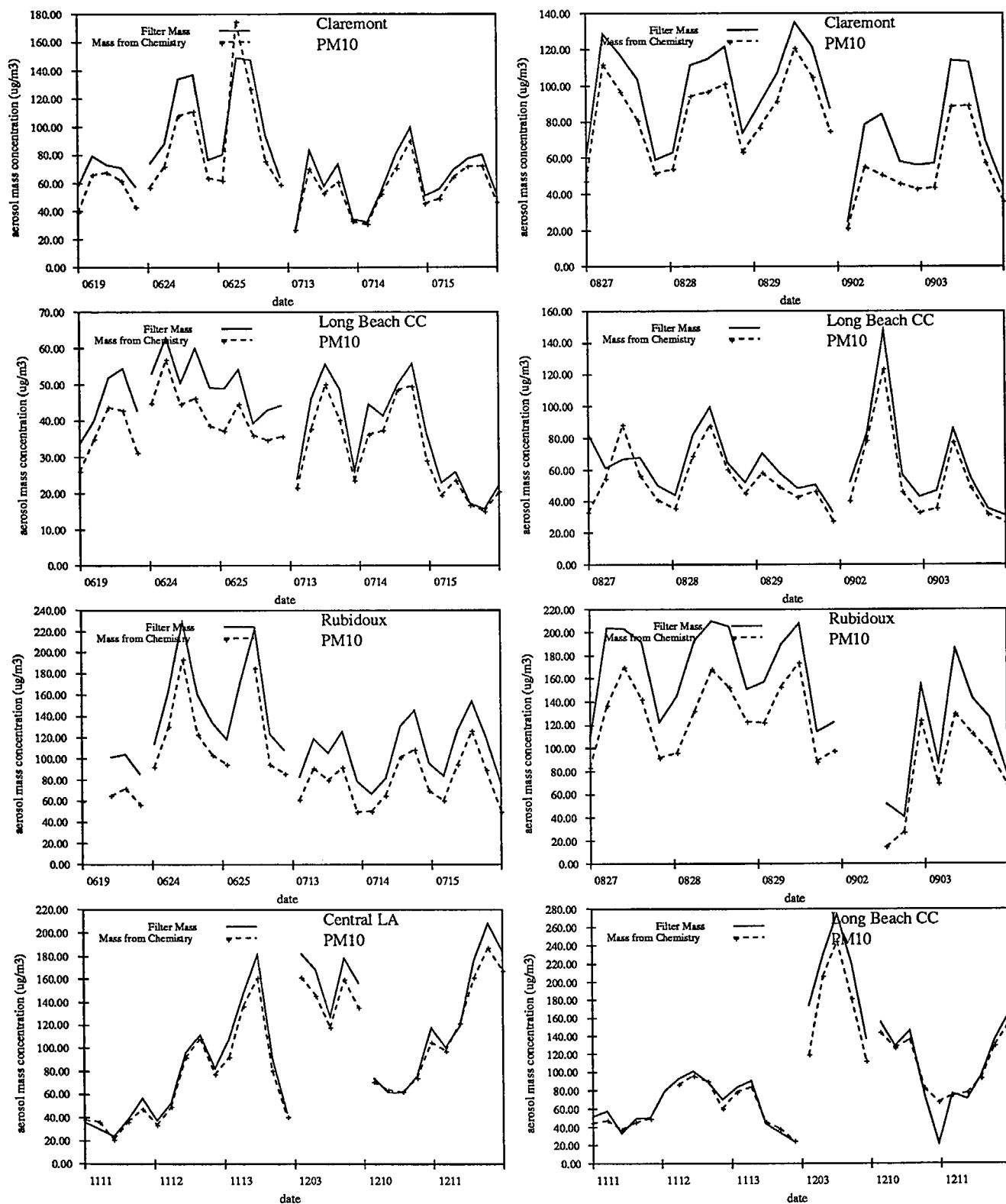


Figure 15: Comparison of gravimetrically determined PM10 mass to the sum of the mass concentrations of identified chemical species.

Table 4: Density and Refractive Index of Chemical Species

<i>Species</i>	oxidized species	density (g/cm ³)	real ref. index	imaginary ref. index
Organic C		1.4	1.55	
Elemental C		2.0	1.9	0.6
NaCl		2.16	1.54	
NH ₄ NO ₃		1.72	1.55	
(NH ₄) ₂ SO ₄		1.77	1.52	
NaNO ₃		2.26	1.59	
Na ₂ SO ₄		2.68	1.48	
NH ₄ HSO ₄		1.78	1.47	
H ₂ SO ₄		2.3	1.53	
Mg	MgO	3.58	1.74	
Al	Al ₂ O ₃	3.96	1.76	
Si	SiO ₂	2.30	1.48	
K	K ₂ O	2.32	1.50	
Ca	CaO	3.25	1.84	
Ti	TiO ₂	4.26	2.62	
Fe	Fe ₂ O ₃	5.24	3.01	
Sr	SrO ₂	4.56	1.6	
Mn	Mn ₂ O ₇	2.40	1.6	
Cu	CuO	6.30	2.63	
Zn	ZnO	5.61	2.01	
Br	Br	2.3	1.53	
V	V ₂ O ₅	3.36	1.46	
Ni	NiO	6.67	2.18	
residue		2.3	1.53	0.005
water		1.0	1.38	

Reference: CRC, 1985; Sloane, 1988

coefficient whose value is nonzero.

In order to facilitate the investigation of the role of water in these atmospheric aerosols, a technique was selected to estimate the amount of water present in the original aerosol. The method used is adapted from Sloane (1984). Using this method, the concentration of soluble aerosol mass is calculated from the chemical composition of the filter samples. The van't Hoff equation is then applied to calculate the water present. The aerosol volume inferred from the filter sample was regressed on the aerosol volume inferred from the aerosol size distribution instruments both with and without addition of aerosol water to the filter sample-based data set in the amounts that were originally present under ambient conditions. The correlation coefficient for the regression of the filter-based aerosol volume data on the size distribution instrument-based aerosol volume data was consistently higher for the case without water addition to the filter data than for the case with water addition to the filters. The above tests suggest that the light scattering coefficient measurements made using heated inlet nephelometers, the optical particle size distribution measurements, and the gravimetric filter measurements made after dessication were all conducted on aerosols that were in similar states of water retention. In short, all of the sampling procedures used apparently dried out the aerosol before measurements were made. Therefore, visibility model verification tests reported here first will compare predicted and measured aerosol scattering at low relative humidity conditions. Then in a second stage of the investigation, an estimate will be made of the amount of light scattering that would occur at the ambient relative humidities that prevailed at the time of sample collection.

5.8 Estimation of Refractive Index

Two methods were used for calculating the aerosol refractive index. In the first method, a volume-averaged refractive index is computed. The aerosol chemical composition data described in section 5.6 were used in conjunction with the density and refractive index information presented in Table 4 to compute refractive index values for the aerosol that are the weighted sum of the refractive indexes of the individual species shown in Table 4.

The weighting factors are the volume fraction contributed by each chemical substance. The second method used is based on the work of Stelson (1990). In this method the refractive index for ionic aerosols is estimated from the sum of the product of partial molar refractive indexes of ionic species and the mole fractions of those ionic species. Partial molar refractive indexes are also defined for non-ionic species such as elemental and organic carbon and some of the trace metal oxides.

To facilitate the examination of the role of aerosol water in these calculations, the refractive index was calculated for two different states of hydration of the aerosol as shown in Table 5. The aerosol water content can be calculated by Sloane’s method only when the ambient relative humidity is known. For this reason, there are fewer time periods when the refractive index can be estimated by methods 2 and 4 of Table 5.

It was found that when using either partial molar refractive indices or volume averaged refractive indices, (methods 1 and 2 of Table 5 versus methods 3 and 4 of Table 5), the differences in the present cases are so small that the two methods produce nearly indistinguishable light scattering results, given the same aerosol size distributions within a Mie scattering calculation.

5.9 Calculation of the Extinction Coefficient

The extinction coefficient can be expressed as the sum of four contributions.

$$b_{ext} = b_{sp} + b_{ap} + b_{sg} + b_{ag} \quad (1)$$

The extinction coefficient is the sum of the components due to light scattering by particles, b_{sp} , light absorption by particles, b_{ap} , scattering of light by gases, b_{sg} , also known as Rayleigh scattering when the gas is air, and light absorption by gases b_{ag} . Light scattering and absorption by particles is calculated from Mie theory . The refractive index values and aerosol size distribution are required to perform the Mie scattering calculation. The scattering and absorption efficiencies are calculated for each diameter interval of the aerosol particle size distribution. Then b_{sp} and b_{ap} are calculated by integrating the product of the

Table 5: Methods Used to Calculate Alternative Refractive Index Values

<i>Method Number</i>	<i>Assumptions</i>
1	volume averaged refractive index computed; with no water present
2	volume averaged refractive index computed; ambient water estimated by method of Sloane
3	partial molar refractive index computed; with no water present
4	partial molar refractive index computed; ambient water estimated by method of Sloane

scattering and absorption efficiency factors for particles of each size and the number of such particles per unit air volume over the diameter range represented by the aerosol size distribution. Light absorption by NO_2 gas is calculated according to the wavelength dependent absorption coefficients reported by Hodkinson (1966) . Scattering by gases is calculated as Rayleigh scattering, with $b_{sg} = 1.5 * 10^{-5} m^{-1}$ at a wavelength of 550 nm, and b_{sg} varying with wavelength as λ^{-4} . These calculations are described in detail by Larson *et al.* (1988).

5.10 Visibility Model Results

Data on the aerosol size distribution and refractive index corresponding to each short term sampling period were supplied to a Mie scattering code using procedures similar to those of Larson *et al.* (1988, 1989). The particle light scattering coefficient, b_{sp} of equation 1, was calculated as a function of wavelength. These results then were compared to values of the particle light scattering coefficient as determined experimentally by the integrating nephelometers.

Three sets of calculations are presented here that will be referred to as cases A, B, and C, as listed in Table 6. These represent a progression from a model based on the raw fine particle data alone (A), to one in which light scattering by dry particles in the diameter range of 2.5 to 10 μm is added to the scattering by dry fine particles (B), to one where the dry fine particle size distribution is corrected to match the aerosol volume inferred from the fine particle filter samples (C). In these calculations, the refractive index of the dry aerosol will be estimated by the volume averaged method (method 2 of Table 5). In each case, calculated scattering by dry particles can be compared to nephelometer measurements of scattering by dry particles at the wavelength of maximum sensitivity of each particular nephelometer.

Results of the model calculations for light scattering by dry fine particles (case A) are shown in time series in Figure 16. Figure 16 shows that light scattering by particles at Claremont is explained quite well based on light scattering by a dry aerosol. Both the magnitude and the temporal trends of the measured light scattering coefficient values are reproduced. In the summer period at Long Beach, the model calculations explain light scattering levels

Table 6: Methods Used to Assign Size Distributions

<i>Case</i>	<i>Size Distribution Description</i>
A	dry fine aerosol size distribution EAA to 0.23 μm , PMS OPC 0.23 to 2.83 μm diameter
B	dry aerosol size distribution extended to 10 μm diameter Case A with constant distribution from 2.5 to 10 μm diameter
C	extended dry aerosol size distribution corrected to match filter data Case B with fine particle distribution scaled to match volume determined from PM2.5 filter samples
D	wetted aerosol Case C with water added to coarse and fine aerosol according to Sloane's method; size distribution scaled up to match computed wet aerosol volume

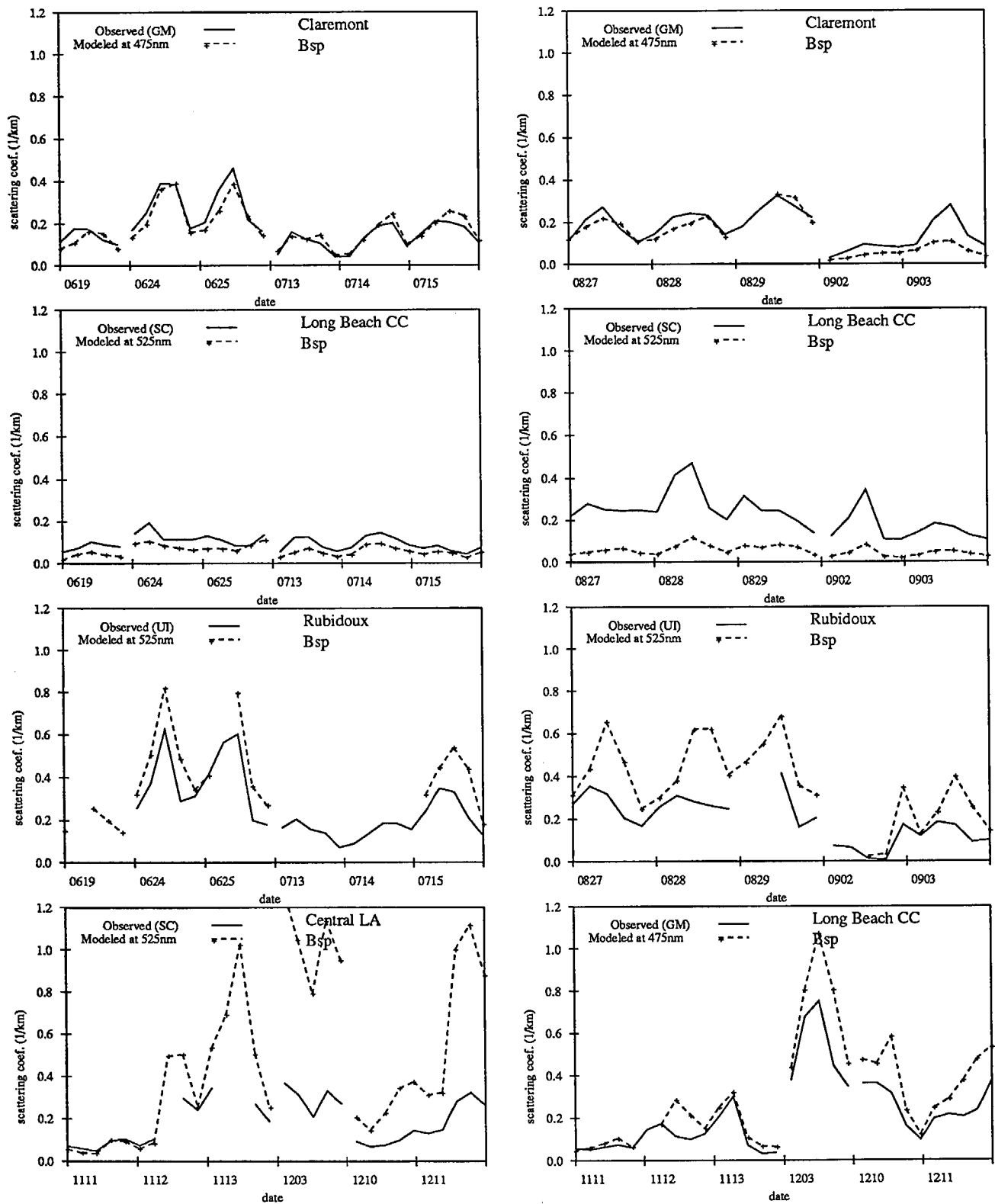


Figure 16: Comparison of calculated light scattering by dry fine particles to nephelometer measurements of the particle light scattering coefficient (Case A).

fairly well during June and July but underpredict the light scattering coefficient in August and September. Long Beach is modeled well in the winter period.

The effect of inclusion of particles in the 2.5 μm to 10 μm size range (Case B) is shown in Figure 17. The addition of particles in the 2.5 to 10 μm diameter range does not noticeably affect the calculated particle light scattering coefficient values. Hence, the model is not particularly sensitive to the approximate size distribution used for particles in this larger size range.

Time series plots in Figure 18 show the results of scaling the aerosol size distribution so that the dry aerosol volume matches that inferred from the filter samples (Case C). This correction produces a major improvement between predictions and observations at Rubidoux. Predictions and observations are still in close agreement at Claremont at all times and at Long Beach in June, July, November, and December. Agreement at Central Los Angeles is improved.

The particle light scattering coefficient values at each site predicted for Cases A, B, and C were regressed on all of the available nephelometer data. The results are shown in Table 7. Results at Claremont show very close to unit slope, zero intercept when compared to both the GM and UI nephelometer data sets. Comparisons to the UI nephelometer data set at Rubidoux and to the GM nephelometer data set at Long Beach (fall) likewise show relatively good agreement. The comparisons against the SCAQS network nephelometers (SC) at Claremont and Long Beach during times when simultaneous nephelometer data were available from other sources show lower correlations with model predictions. Poor agreement between measurements and model results occur only in those cases (Long Beach summer, Central LA winter) where a single SC nephelometer is present with no possibility of comparison against a second instrument.

Next, water addition to the aerosol was simulated (approximately) in order to explore the likely level of light scattering by the aerosol under ambient conditions. The refractive index of the wet aerosol was estimated by the volume averaged method with water included (method 2 of Table 5). Calculated light scattering by the humidified aerosol (Case D) is

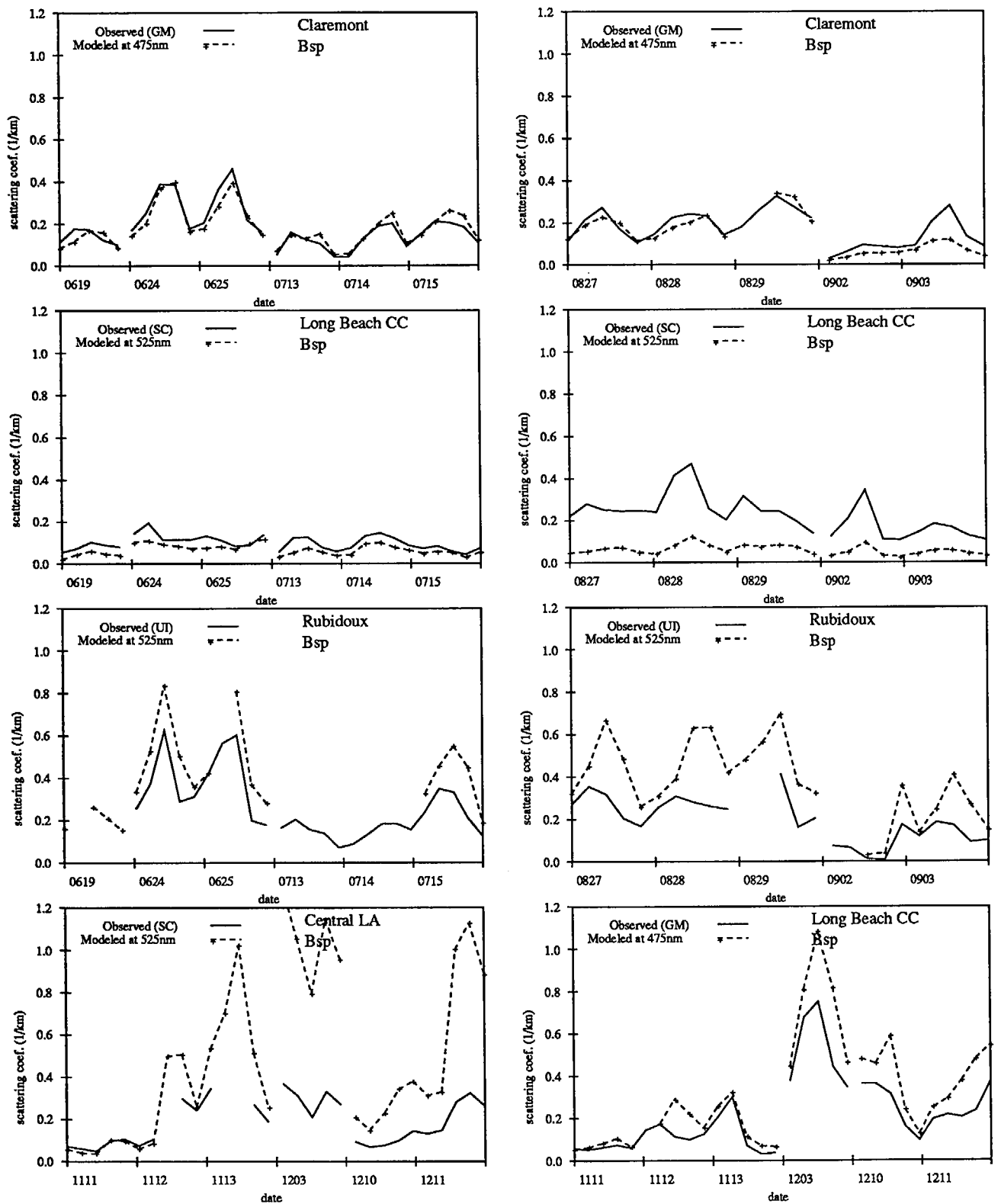


Figure 17: Comparison of calculated light scattering by dry particles of $10 \mu\text{m}$ diameter and smaller to nephelometer measurements of the particle light scattering coefficient (Case B).

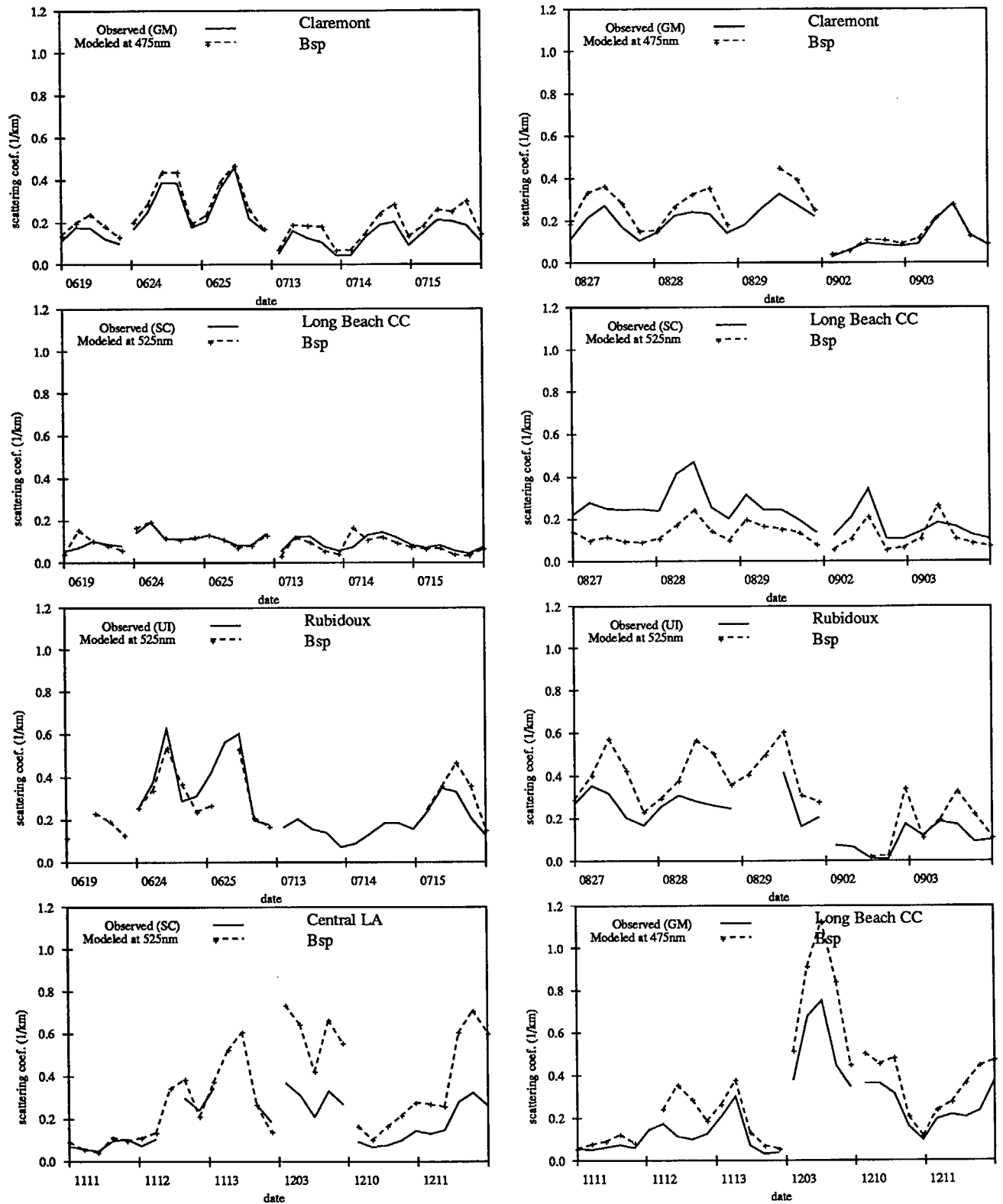


Figure 18: Comparison of calculated light scattering by particles to nephelometer measurements of the particle light scattering coefficient after having corrected the aerosol volume distributions to match the aerosol volume inferred from simultaneous filter samples (Case C).

Table 7: Regression of Modeled Light Scattering Coefficient Values on Nephelometer Measurements of the Light Scattering Coefficient (all data)

Predicted = α Observed + β							
Site and Nephelometer	Case	alpha	(std err)	beta	(std err)	n	correlation coefficient (r)
<i>summer</i>							
Claremont SC	A	1.172	(0.102)	0.015	(0.015)	53	0.850
Claremont SC	B	1.194	(0.103)	0.019	(0.015)	53	0.852
Claremont SC	C	1.520	(0.095)	0.029	(0.014)	53	0.914
Claremont GM	A	0.874	(0.059)	0.030	(0.012)	53	0.900
Claremont GM	B	0.893	(0.058)	0.033	(0.011)	53	0.908
Claremont GM	C	1.113	(0.050)	0.050	(0.010)	53	0.952
Claremont UI	A	0.886	(0.056)	0.009	(0.011)	52	0.913
Claremont UI	B	0.906	(0.055)	0.012	(0.011)	52	0.918
Claremont UI	C	1.099	(0.058)	0.030	(0.011)	52	0.937
Long Beach CC SC	A	0.120	(0.032)	0.058	(0.006)	55	0.457
Long Beach CC SC	B	0.124	(0.033)	0.062	(0.006)	55	0.463
Long Beach CC SC	C	0.379	(0.056)	0.069	(0.010)	55	0.681
Rubidoux UI	A	1.177	(0.140)	0.101	(0.040)	36	0.822
Rubidoux UI	B	1.192	(0.140)	0.109	(0.040)	36	0.824
Rubidoux UI	C	0.804	(0.138)	0.125	(0.039)	36	0.708
<i>fall</i>							
Central LA SC	A	3.340	(0.373)	-0.135	(0.080)	27	0.873
Central LA SC	B	3.357	(0.375)	-0.135	(0.080)	27	0.873
Central LA SC	C	1.873	(0.203)	-0.019	(0.043)	27	0.879
Long Beach CC SC	A	1.629	(0.255)	-0.065	(0.065)	29	0.776
Long Beach CC SC	B	1.642	(0.256)	-0.062	(0.065)	29	0.777
Long Beach CC SC	C	1.786	(0.235)	-0.087	(0.060)	29	0.826
Long Beach CC GM	A	1.352	(0.079)	0.043	(0.023)	29	0.957
Long Beach CC GM	B	1.357	(0.079)	0.047	(0.023)	29	0.957
Long Beach CC GM	C	1.400	(0.074)	0.047	(0.022)	29	0.964

compared to the time series of dry aerosol scattering (Case C) in Figure 19. It is seen that the effect of humidifying the aerosol is relatively small except for certain time periods at Rubidoux, and at Long Beach during the fall period.

Finally, light absorption by NO_2 , light absorption by black carbon particles, and light scattering by air molecules were added to the light scattering by particles in order to compute the total extinction coefficient according to equation 1. Results shown in Figures 20 – 23 indicate that light scattering by fine particles dominates the visibility problem at each monitoring site. Light absorption by black carbon particles makes an increasingly important contribution to the extinction coefficient in the fall and winter months at Long Beach and Central Los Angeles.

5.11 Conclusions

Aerosol size distribution data and filter based measurements of aerosol chemical composition were collected during the summer and fall of 1987 by the SCAQS air monitoring network. A visibility model has been constructed that uses these data to calculate aerosol light scattering coefficient values in time series at four air monitoring sites from Mie theory.

A set of consistency checks were performed on the aerosol data base. The measured aerosol anions and cations were found to be in close agreement. The gravimetrically determined aerosol mass concentrations were compared to the sums of the mass concentrations of identified chemical species, and again reasonable agreement was found between these two data sets. A high correlation also was found between the aerosol volume measured by the aerosol size distribution instruments and the aerosol volume inferred from the filter samples. Hence, it is concluded that the SCAQS aerosol data base displays sufficient internal consistency to be used for the purpose of the present visibility model study. The light scattering coefficient values measured during SCAQS by different monitoring agencies were not always in agreement. For that reason, no visibility model can be expected to produce exact agreement with all measured light scattering values because the light scattering data are in conflict to some degree.

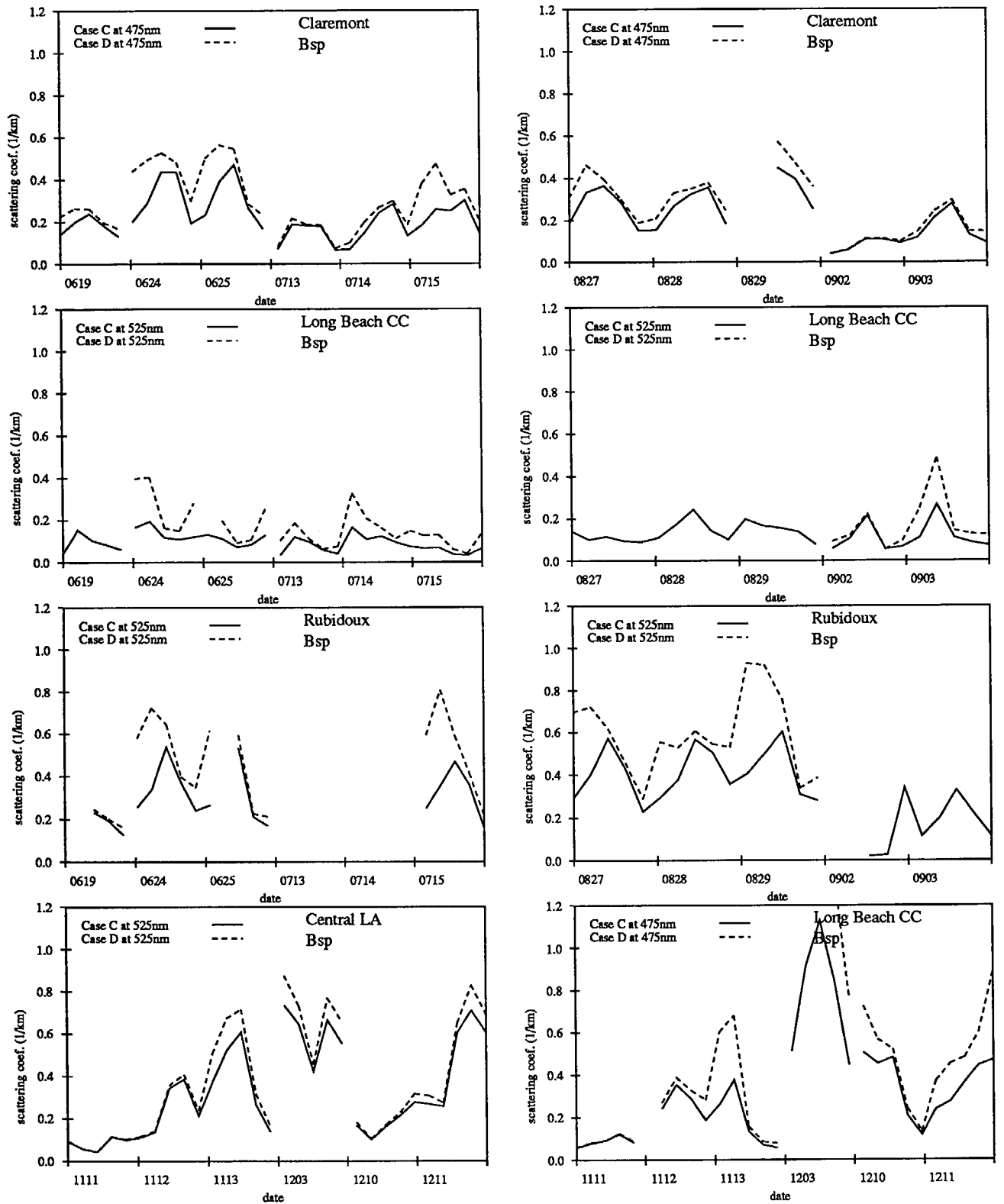


Figure 19: Comparison of light scattering computed for a dry aerosol (Case C) to light scattering by a wetted aerosol (Case D).

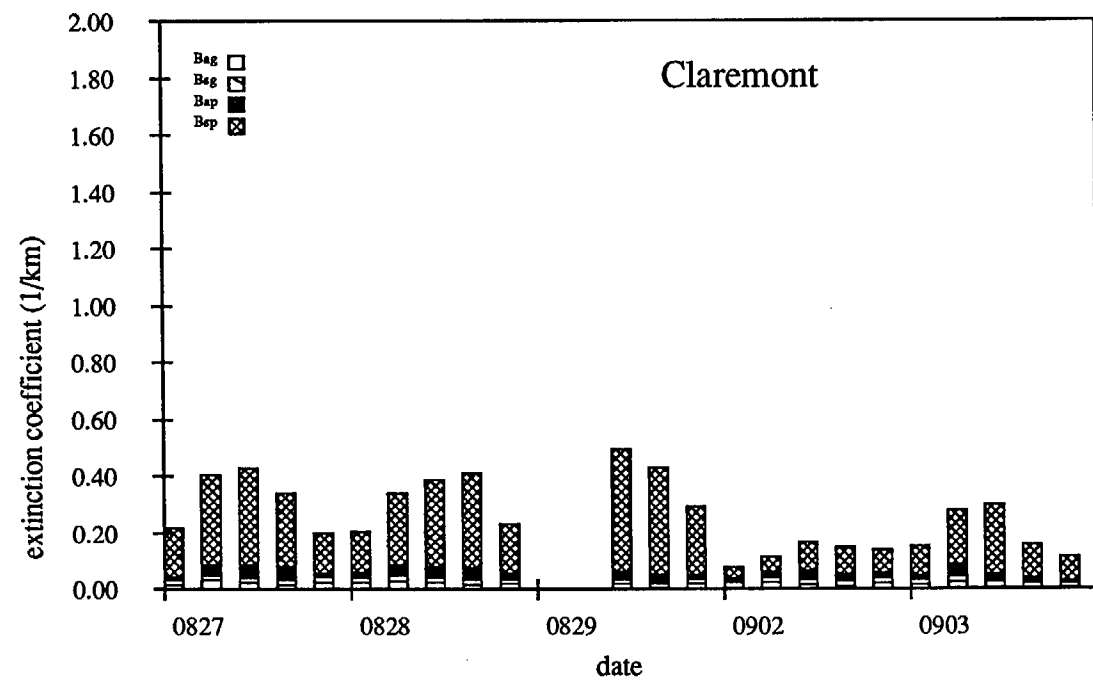
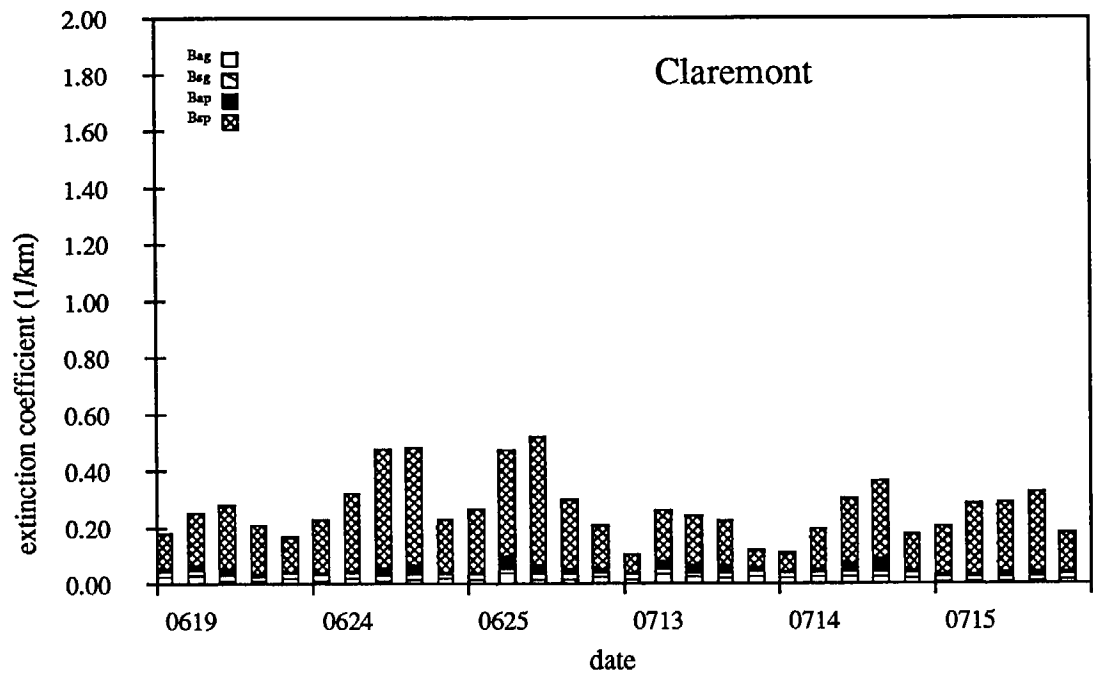


Figure 20: Calculated values of the total light extinction coefficient for the Claremont site (Case C).

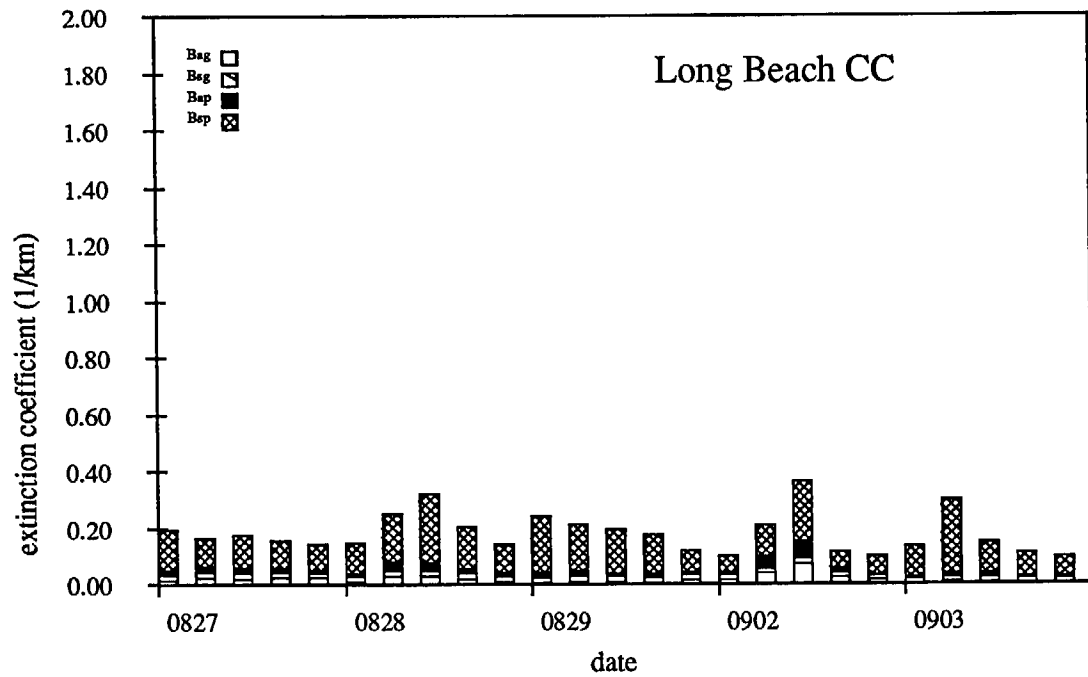
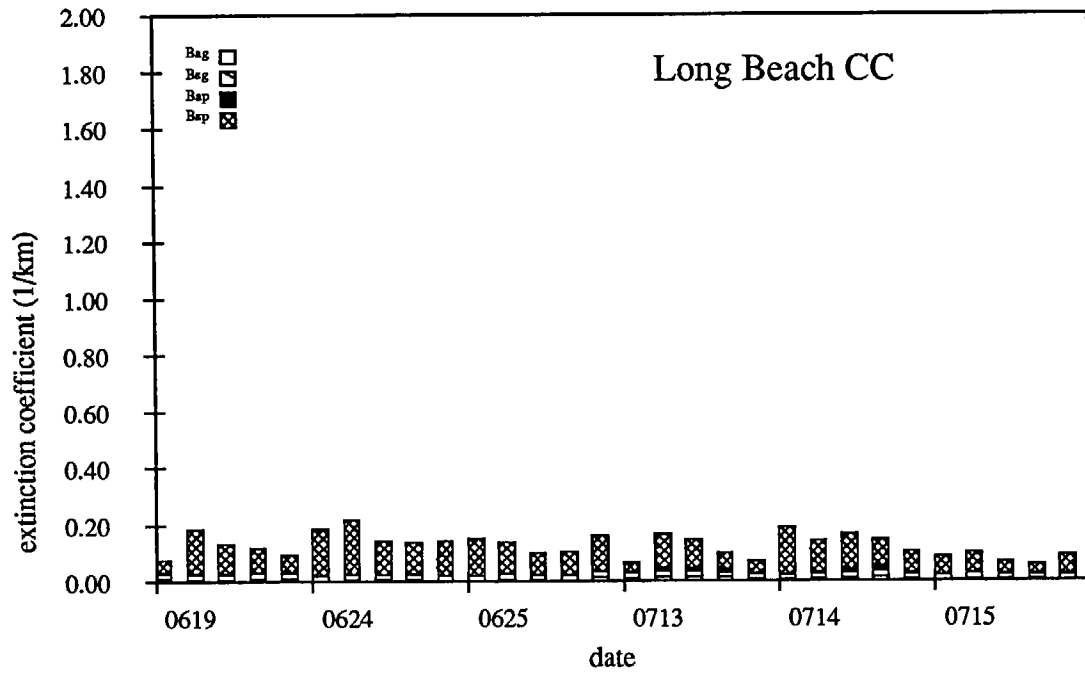


Figure 21: Calculated values of the total light extinction coefficient for the Long Beach CC site (Case C).

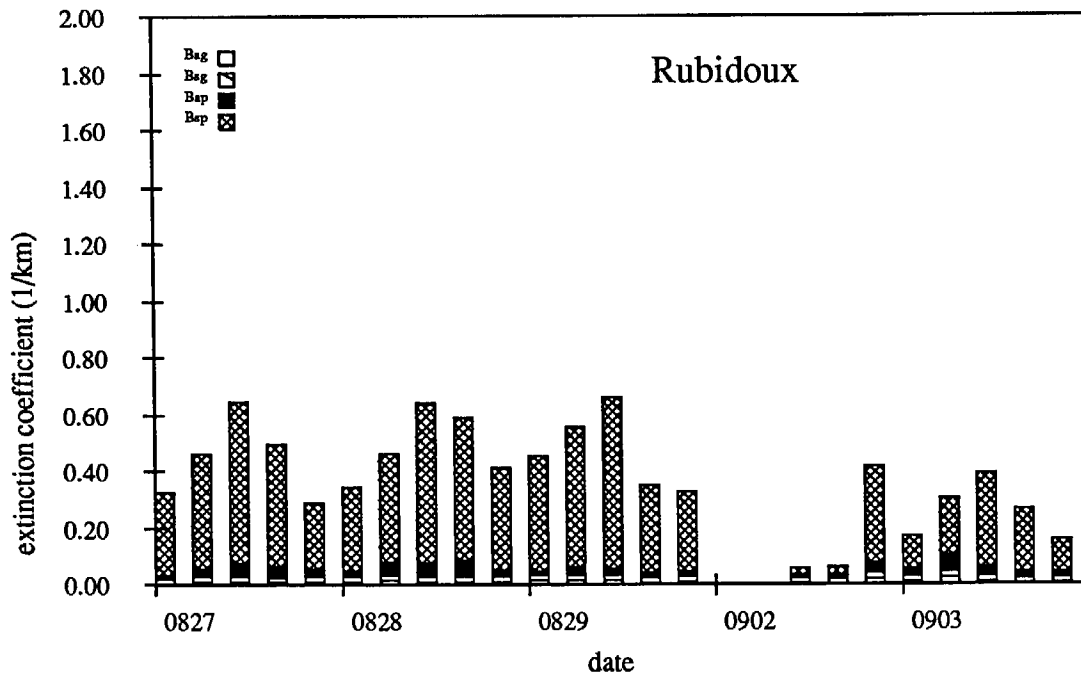
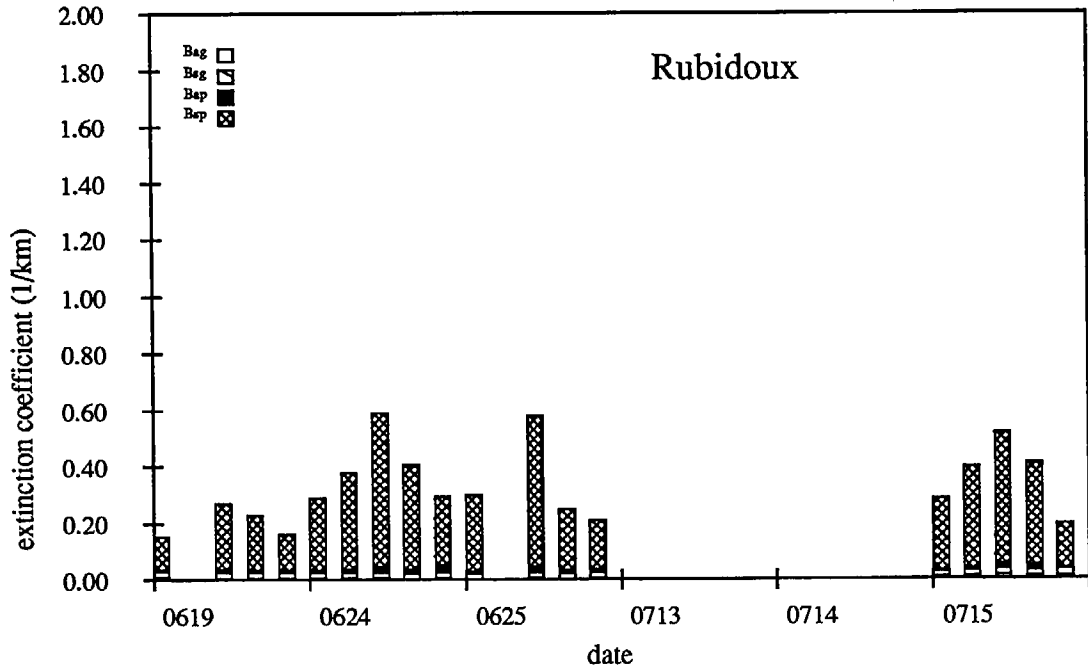


Figure 22: Calculated values of the total light extinction coefficient for the Rubidoux site (Case C).

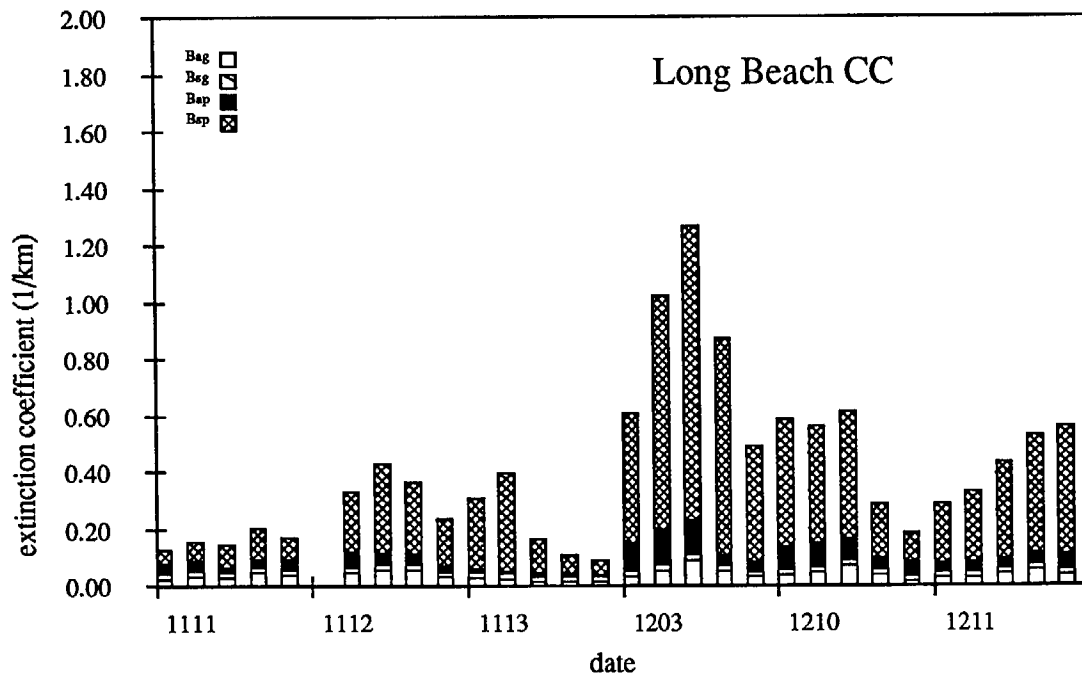
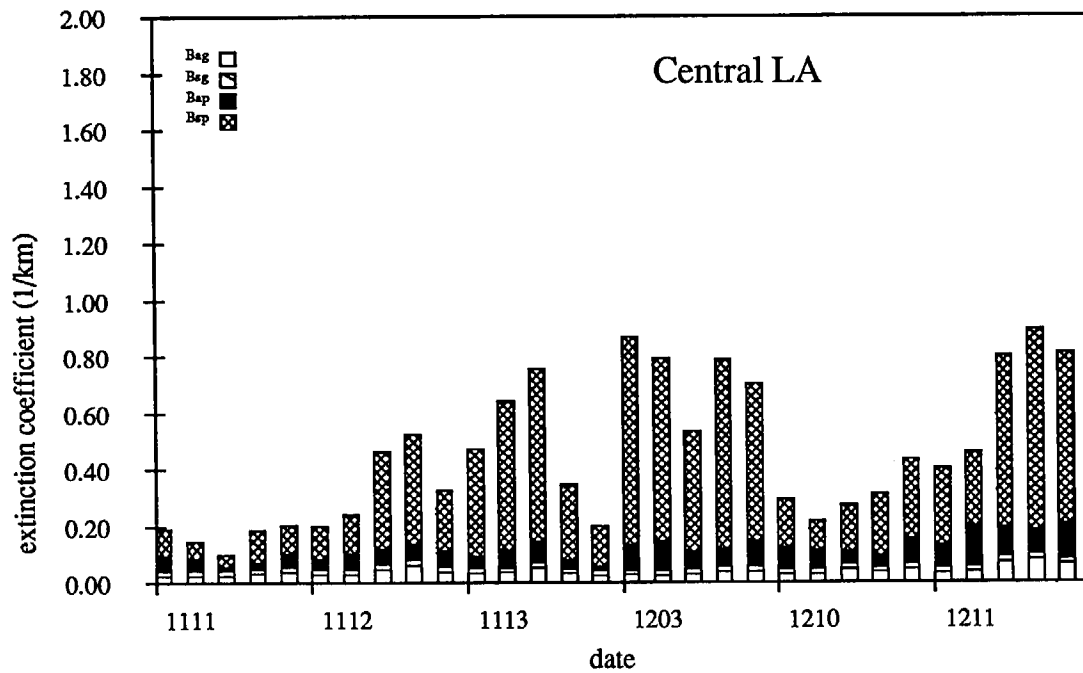


Figure 23: Calculated values of the total light extinction coefficient for the Central LA and Long Beach CC sites in the fall (Case C).

The light scattering coefficient values calculated from the visibility model were found to reproduce the time series of measured light scattering coefficient values well in the case where redundant nephelometer measurements were available at a particular air monitoring site. Total light extinction coefficient values, which can be easily converted to estimates of standard visual range via Koschmeider's formula, also were computed at each monitoring station. Based on this study, it appears practical to maintain a network of monitoring sites that can be used to track the relationship between pollutant properties and visual range via modeling calculations based on Mie theory.

References

- [1] Appel, B. R., Wall, S. M., Tokiwa, Y., and Haik, M. (1980), Simutaneous nitric acid, particulate nitrate and acidity measurements in ambient air. *Atmospheric Environment*, **14**, 549-554.
- [2] Blumenthal, D. L., Watson, J., and Lawson, D. (June 1986). *Southern California Air Quality Study Suggested Program Plan*. Technical Report, California Air Resources Board, Sacramento, California 95812.
- [3] Cass, Glen R. (1979), On the relationship between sulfate air quality and visibility with examples in Los Angeles. *Atmospheric Environment*, **13**, 1069-1084.
- [4] Chan, Michael and Durkee, Kevin. (April 1989). *Southern California Air Quality Study B-Site Operations*. Technical Report contract A5-196-32, Aerovironment, Inc., Monrovia, California 91016.
- [5] Fitz, D., Chan, M., Cass, G., Lawson, D., and Ashbaugh, L. (1989). A multi-component size-classifying aerosol and gas sampler for ambient air monitoring. Air and Waste Management Association paper 89-140.1.
- [6] Gray, H. Andrew, Cass, Glen R., Huntzicker, James J., Heyerdahl, Emily K., and Rau, John A. (1986), Characteristics of atmospheric organic and elemental carbon particle concentrations in Los Angeles. *Environmental Science and Technology*, **20**, 580-589.
- [7] Hering, S. V. and Blumenthal, D. L. (December 1989). *Southern California Air Quality Study Description of Measurement Activities, Final Report*. Technical Report contract A5-157-32, California Air Resources Board, Sacramento, California 95812.
- [8] Hering, S. V. and others,. (1988), The nitric acid shootout: field comparison of measurement methods. *Atmospheric Environment*, **22**, 1519-1539.

- [9] Hering, Susanne. (July 1990). *Southern California Air Quality Study Aerosol Data Management Report, Final Report*. Technical Report contract A832-086, California Air Resources Board, Sacramento, California 95812.
- [10] Hering, Susanne V. and McMurry, Peter H. (1991), Optical counter response to monodisperse atmospheric aerosols. *Atmospheric Environment*, **25A(2)**, 463–468.
- [11] Hodkinson, J. Raymond. (1966), Calculations of colour and visibility in urban atmospheres polluted by gaseous NO_2 . *Air and Water Pollut. Int. J.*, **10**, 137.
- [12] John, Walter, Wall, Stephen M., Ondo, Joseph L., and Winklmayr, Wolfgang. (1990), Modes in the size distribution of atmospheric inorganic aerosol. *Atmospheric Environment*, **24A**, 2349–2359.
- [13] Larson, Susan M. and Cass, Glen R. (1989), Characteristics of summer midday low-visibility events in the Los Angeles area. *Environmental Science and Technology*, **23**, 281–289.
- [14] Larson, Susan M., Cass, Glen R., Hussey, Kevin J., and Luce, Frederick. (1988), Verification of image processing based visibility models. *Environmental Science and Technology*, **22**, 629–637.
- [15] Matsumura, Robert T. and Cahill, Thomas A. (January 1991). *Spatial Inhomogeneities in SCAQS Filters*. Technical Report contract A832-128, California Air Resources Board, Sacramento, California 95812.
- [16] Middleton, W. E. (1952). *Vision Through the Atmosphere*. University of Toronto Press.
- [17] Penndorf, Rudolf. (1957), Tables of the refractive index for standard air and the Rayleigh scattering coefficient for the spectral region between 0.2 and 20.0μ and their application to atmospheric optics. *Journal of the Optical Society of America*, **47**, 176–182.

- [18] Rood, M. J., Covert, D. S., and Larson, T. V. (1987), Temperature and humidity controlled nephelometry: improvements and calibration. *Aerosol Science and Technology*, **7**, 57-65.
- [19] Ruby, Micheal G. and Waggoner, Alan P. (1981), Intercomparison of integrating nephelometer measurements. *Environmental Science and Technology*, **15**, 109-113.
- [20] Sloane, Christine S. *Fortran Algorithm for the Calculation of Light Scattering by Stratified Spheres*. 1984. General Motors Research Laboratories, Warren, Michigan, RM 11-70.
- [21] Sloane, Christine S. (1984), Optical properties of aerosols of mixed composition. *Atmospheric Environment*, **18**, 871-878.
- [22] Solomon, P. A., Larson, S. M., Fall, T., and Cass, G. R. (1988), Basinwide nitric acid and related species concentrations observed during the Claremont nitrogen species comparison study. *Atmospheric Environment*, **22**, 1587-1594.
- [23] Stelson, Arthur W. (1990), Urban aerosol refractive index prediction by partial molar refraction approach. *Environmental Science and Technology*, **24**, 1676-1679.
- [24] Stelson, Arthur W. and Seinfeld, John H. (1981), Chemical mass accounting of urban aerosol. *Environmental Science and Technology*, **15**, 671-679.
- [25] Trijonis, John. (July 1980). *Visibility in California*. Technical Report contract A7-181-30, Technology Service Corporation, Santa Monica, California 90405.
- [26] Wall, Stephen M., John, Walter, and Ondo, Joseph L. (1988), Measurements of aerosol size distributions for nitrate and major ionic species. *Atmospheric Environment*, **22**, 1649-1656.
- [27] Weast, Robert C., editor. *CRC Handbook of Chemistry and Physics*, pages B67-B161. CRC Press, 66th edition(1985).

- [28] Whitby, Kenneth H. and Sverdrup, George. California aerosols: their physical and chemical characteristics. In Hidy *et al.*, G. M., editor, *The Character and Origins of Smog Aerosols*, John Wiley and Sons(1980).
- [29] White, W. H. and Roberts, P. T. (1977), On the nature and origins of visibility-reducing aerosols in the Los Angeles air basin. *Atmospheric Environment*, **11**, 803–812.

A Correction factors applied to the PMS OPC data

Table A: Diameter Corrections Applied to PMS OPC Data according to experiments of Hering and McMurry (1991)

<i>Reported Diam.</i>	<i>Corrected Diam.</i>	D_{corr}/D_{orig}
0.235	0.240	1.02
0.263	0.290	1.10
0.295	0.345	1.17
0.330	0.396	1.20
0.369	0.469	1.27
0.413	0.553	1.34
0.463	0.648	1.40
0.518	0.720	1.39
0.580	0.770	1.33
0.649	0.805	1.24
0.727	0.858	1.18
0.815	0.905	1.11
0.912	0.960	1.05
1.021	1.06	1.04
1.143	1.18	1.03
1.280	1.30	1.02